The Thesis committee for Stephen Douglas Riutta

certifies that this is the approved version of the following thesis:

Contributions of muscles to body segment energetics during the squat jump

APPROVED BY

SUPERVISING COMMITTEE:

Supervisor: ______________________

Ashish D. Deshpande

____

Jonathan Dingwell

Contributions of muscles to body segment energetics during the squat jump

by

Stephen Douglas Riutta, B.S.

THESIS

Presented to the Faculty of the Graduate School of

The University of Texas at Austin

in Partial Fulfillment

of the Requirements

for the Degree of

Master of Science in Engineering

THE UNIVERSITY OF TEXAS AT AUSTIN

August 2014

Dedicated to my supportive parents, family, and friends.

Acknowledgments

I would like to acknowledge the support from the members of the Rehabilitation and Neuromuscular (ReNeu) Robotics lab. I would also like to acknowledge the contributions from Tom Ordelt and the University of Maine in collecting the experimental data. I would also like to thank Dr. Jonathan Dingwell for the early discussions that helped to guide the focus of the research. Finally, I appreciate the insightful discussions and support from my advisor, Dr. Ashish D. Deshpande.

Contributions of muscles to body segment energetics during the squat jump

by

Stephen Douglas Riutta, M.S.E.
The University of Texas at Austin, 2014

SUPERVISOR: Ashish D. Deshpande

Despite the squat jump's intriguing dynamical properties and prevalence in athletics, there is a lack of information regarding the comprehensive functional role of muscles during the squat jump. To increase our understanding of the strategies the human body uses in accelerating joints and contributing energy to body segments, we incorporated experimental data from trained collegiate men and women into musculoskeletal computer simulations. We evaluated the simulations to determine fundamental coordination principles of the squat jump, and the effect of increased loading and gender on muscle strategies employed during the squat jump. Our results revealed that the plantar flexors and vasti were primarily involved in increasing the mechanical energy of the body, while the proximal muscles were primarily involved in redistributing energy throughout the body. The erector spinae muscles extended the lumbar spine, and contributed energy to the torso, while gluteus maximus and hamstrings extended the hip joint, and contributed energy to the pelvis.

The vasti extended the knee joint, and contributed energy to the pelvis and torso. Our results suggested that the rectus femoris plays a critical role in converting rotational energy into vertical kinetic energy. Greater barbell loads reduced the rate of lumbar extension, and resulted in increased normalized energy contributions from soleus and vasti to the torso. When comparing the squat jumps between men and women, our results suggested that soleus and vasti are more active in men than women during the body-weight squat jump.

Table of Contents

List of Tables

List of Figures

Chapter 1

Introduction

The squat jump's widespread prevalence in athletics and intriguing dynamical properties have led researchers to seek to identify the underlying musculoskeletal coordination principles behind the squat jump's smooth, efficient motion. Through the analysis of experimental kinematic data, some researchers have reported that a major coordination feature of the squat jump is the transfer of mechanical energy from proximal muscles to distal joints via biarticular muscles (Schenau *et al.*, 1987; Gregoire *et al.*, 1984). While the analysis of experimental squat jump data yields plausible coordination hypotheses, this approach is unable to provide the quantitative basis for these claims.

Through the incorporation of experimental data into musculoskeletal models of the leg, researchers have shown that biarticular muscles transfer energy from proximal muscles to distal joints (Bobbert *et al.*, 1986). Similar modeling approaches have also shown that the muscles in the thigh are coordinated in a reciprocal energy-transferring relationship during the squat jump (Jacobs *et al.*, 1996). Although these localized studies have increased our understanding of the functional role of muscles in coordinated movement, it is critical to identify the role of the muscle in the context of the whole body because of the effects of dynamic coupling.

Simulations with whole-body models have supported the claims from earlier studies by showing that biarticular muscles are involved in transferring energy to the distal joints (van Soest & Bobbert, 1993; Bobbert & van Zandwijk, 1994). To date, Pandy & Zajac (1991) have presented the most comprehensive understanding of the coordination principles involved in the human body during the squat jump. In their simulation, muscles were activated in a proximal to distal sequence, and the vasti (VAS) and gluteus maximus (GMAX) were the greatest power contributors to the torso. However, while Pandy & Zajac (1991) provided insights into muscular and segmental energetics, the lack of a lumbar joint and torso muscles in their model may lead to misinterpretations of the functional role of muscles. Further, while their simulation reproduced many of the experimental squat jump features, it also showed an increase in the angular speed of the segments at lift-off. Finally, their study did not identify the whole-body role of the muscles in generating, absorbing, and redistributing energy in the body.

The objective of our study was to obtain a comprehensive understanding of the functional role of muscles in generating, absorbing, and transferring energy among body segments during the squat jump. We achieved this objective by incorporating experimental ground reaction forces and motion data from trained collegiate athletes into anthropometrically-scaled, 8-segment, 3D musculoskeletal models to create computer simulations of the squat jump. We evaluated the functional role of muscles across a range of barbell masses, and between genders to determine the response of muscles to external perturbations, and to ensure that our simulation results were robust to kinetic and geometric changes. Specifically, we hypothesized that 1) Biarticular muscles would transfer more energy among body segments than they generated, 2) Increased loading would result in new muscular strategies, and 3) Anthropometric and muscle composition differences between men and women would lead to different muscular strategies across the range of barbell masses.

Chapter 2

Materials and Methods

We measured marker positions, electromyographic (EMG) data, and ground reaction forces from seven female collegiate athletes (mass 59.4±4.53 kg, one squat repetition maximum 100.7± kg, height 1.67±0.07 m) and five male collegiate athletes (mass 78.4±11.0 kg, one squat repetition maximum 137.5±24.3 kg, height 1.81±0.04 m) as they performed a total of 97 (40 male, 57 female) squat jumps with barbell masses ranging from 0 - 50% of their one repetition maximums (1RM). The ground reaction forces and marker trajectories were incorporated into subject-specific musculoskeletal models to generate simulations of the squat jump.

2.1 Experimental protocol

The study was approved by the Institutional Review Board of the University of Maine, and each subject signed an informed consent form. The subjects were given a period of time to warm up, and executed the prescribed exercises. A 90° angle at the knee joint at the lowest point of the squat jump was maintained for all subjects by placing an elastic band below the subject at the appropriate height. The subjects were given sufficient time to rest between trials.

2.2 Experimental data

2.2.1 Ground reaction forces

Ground reaction forces were measured throughout the duration of the squat jump with a calibrated digital scale (2000 Hz, Arlyn Scales, Model 30M-36). The center of pressure of each foot was recorded with Tekscan F-Scan pressure sole sensors at 100 Hz. The force data from the digital scale and the pressure soles was synchronized with the motion of the model by aligning their force peaks with peaks produced by the acceleration of the center of mass of the model. The sole pressure was converted to force by multiplying it by the area of each pressure cell, and the sum of the forces on each foot was scaled to equal the total force values recorded from the force plate. The anterior-posterior shear forces, and the distribution of the vertical forces on the left and right feet were estimated using whole body angular momentum:

$$\vec{H} = \sum_{i=1}^{n} [(\vec{r}_i^{COM} - \vec{r}_{body}^{COM}) \times m_i(\vec{v}_i^{COM} - \vec{v}_{body}^{COM}) + I_i\vec{\omega_i}] \tag{2.1}$$

where $\vec{r}_i^{COM}$ and $\vec{v}_i^{COM}$ are the location and velocity of the center of mass of the ith body segment respectively, $\vec{r}_{body}^{COM}$ and $\vec{v}_{body}^{COM}$ are the location of the center of mass of the whole body respectively, m_i, I_i, and $\vec{\omega_i}$ are the mass, mass moment of inertia, and angular velocity of the of the ith segment respectively. Taking the derivative of $\vec{H}$ yielded the moment, $\vec{M}$ of the body. The moment about the anterior-posterior axis was then used to estimate the vertical force on the left foot:

$$F_{ly} = \frac{M_x + F_{y,total} d_r}{d_r + d_l} \tag{2.2}$$

where F_{ly} was the force on the left foot, M_x is the moment about the sagittal-transverse axis, $F_{y,total}$ is the total vertical force from the digital scale, and d_r and d_l are the distances from the center of mass to the right and left feet along the coronal-transverse axis, respectively. The force on the right foot, F_{ry} was the difference between the total force $F_{y,total}$ and the force on the left foot F_{ly}. The moment about the coronal-transverse axis was used to calculate the shear forces in the direction of the sagittal-transverse axis:

$$F_{shear,total} = \frac{M_z - F_{ry} d_{xr} - F_{ly} d_{xl}}{y_{COM}} \tag{2.3}$$

where $F_{shear,total}$ represents the total shear force in the direction of the sagittal-transverse axis, M_z was the moment about the coronal-transverse axis, F_{ry} and F_{ly} are the vertical forces on the left and right feet respectively, $d_x r$ and $d_x l$ are the distances between the body's COM and the center of pressure on the right and left feet in the direction of the sagittal-transverse axis. The shear force on the left foot was calculated with the total shear force:

$$F_{lx} = \frac{-M_y + F_{shear,total} d_r}{d_r + d_l} \tag{2.4}$$

where F_{lx} was the shear force on the left foot, M_y was the moment about the sagittal-transverse axis, and d_r and d_l are the distances from the center of mass to the right and left feet along the coronal-transverse axis, respectively.

2.2.2 Motion capture

Eight infrared Vicon Nexus cameras captured motion data at 250 Hz from 27 retroreflective markers. The markers were attached to joints and bony prominences on the head, torso, pelvis, thighs, shanks, and feet.

2.2.3 Electromyographic (EMG) data

Electrical muscle activity was recorded from the vastus lateralis (VL), gluteus maximus (GMAX), rectus femoris (RF), and biceps femoris (BF) on both the right and left legs (2000 Hz, Delsys Inc.). The EMG data was high-pass filtered with a 4th order Butterworth filter (40 Hz), demeaned, rectified, and low pass filtered with a zero-lag Butterworth filter (4 Hz).

2.3 Musculoskeletal model

A previously-developed OpenSim musculoskeletal model was used in the analysis (Delp *et al.*, 2007). The model had 19 degrees of freedom, and was actuated by 92 Hill-type musculotendon units. The barbell was modeled by rigidly attaching a point mass to the rear shoulder region of the torso. The mass of the point mass was set to equal the mass of the barbell in each trial. The total mass of the musculoskeletal model was set equal to the mass of each subject, and the physical dimensions of the model were scaled to match the anthropometric measurements of the subjects. The total mass was distributed among the segments of the body based upon the relative physical dimensions of each segment. Each segment was scaled by adjusting the size of the segment until the distance between the model's markers and subject's markers was minimized.

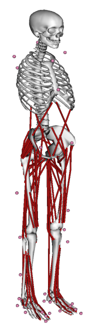

Figure 2.1: Eight-segment, 19 degree-of-freedom musculoskeletal model.

2.4 Data analysis

The OpenSim 'inverse kinematics' tool was used to convert the marker trajectories into rotations and translations of the joints of the musculoskeletal model. The tool minimized the weighted square of the errors between the position of the markers and the location of the corresponding markers on the model. Markers attached to locations such as the pelvis, knee, and ankle were weighted more heavily than those attached to areas subject to motion artifacts. The joint kinematics were filtered with a zero-lag 4th order 7 Hz low-pass Butterworth filter. The 'inverse dynamics' tool was used to calculate the joint moments resulting from the ground reaction forces and motion of the model. The 'static optimization' tool was used to estimate the muscle forces. The tool minimized the sum of the muscle activations required to produce the necessary joint torques. The muscles were constrained with force-length and force-velocity relationships. The 'body kinematics' tool was used to calculate the translational and angular positions of each segment of the model. The 'point kinematics' tool was used to calculate the position of the heel for the pressure sole alignment.

The center of pressure from the pressure-sensitive shoe soles was calculated and was aligned with each foot with rotation matrices.

Whole body power was calculated as $P_{whole} = F_{total}V_{COM}$ where V_{COM} represents the velocity of the center of mass of the model, and F_{total} represents the total ground reaction force. Joint power was calculated as $P_{joint} = M_{joint}\theta_{joint}$ while muscle power was calculated as $P_{muscle} = F_{muscle}V_{muscle}$.

Muscle-induced joint accelerations and muscle contributions of power to segments were calculated with the OpenSim Pseudo-Inverse Induced Acceleration Analysis Plug-In (`simtk.org/home/tims_plugins`). The plug-in used a ground-contact model with five contact points, and implemented previously-developed state-space energy techniques into the OpenSim framework. (Dorn *et al.*, 2012a,b; Lin *et al.*, 2011; Fregly & Zajac, 1996). To determine the whole-body effects of induced accelerations and the flow of energy, the actions of the muscles on the right side of the body were analyzed. The actions of the 46 muscles on the right side of the body were combined into the following groups:

erector spinae (ERCSPN), rectus femoris (RF), the vasti (VAS), soleus (SOL), medial and lateral gastrocnemius (GAS), the hip adductors (ADD), quadriceps femoris (QF), gluteus maximus (GMAX), sartorius (SAR), biceps femoris short head (BFSH), internal obliques (INTBL), the hamstrings muscle group (HAM), and all other muscles (AO).

While the complete phase of the squat jump was recorded, we analyzed the period of time from the lowest point of the COM during the squat jump to the lift-off.

2.5 Statistical analysis

A one-way ANOVA was used to determine whether there were significant differences among the normalized results produced from the 0% 1RM, 25% 1RM, and 40% 1RM squat jumps. If a significant difference existed, Tukey's post-hoc analysis was used to determine which values were statistically significant from one another. The significance level was set to 0.01.

Chapter 3

Results

3.1 Male athletes

3.1.1 Contributions of muscles to segmental energetics during the body-weight squat jump

ERCSPN functioned primarily to extend the lumbar joint (Figure 3.2), thereby contributing energy to the segment (Figure 3.1). This action favorably extended the knee joint, but also unfavorably flexed the hip joint, and decreased the energy of the pelvis. HAM was the primary antagonist to ERCSPN, and extended the hip joint, thereby increasing the energy of the pelvis. However, this action flexed the lumbar joint, thus decreasing the energy of the torso. It also unfavorably dorsiflexed the heel into the ground.

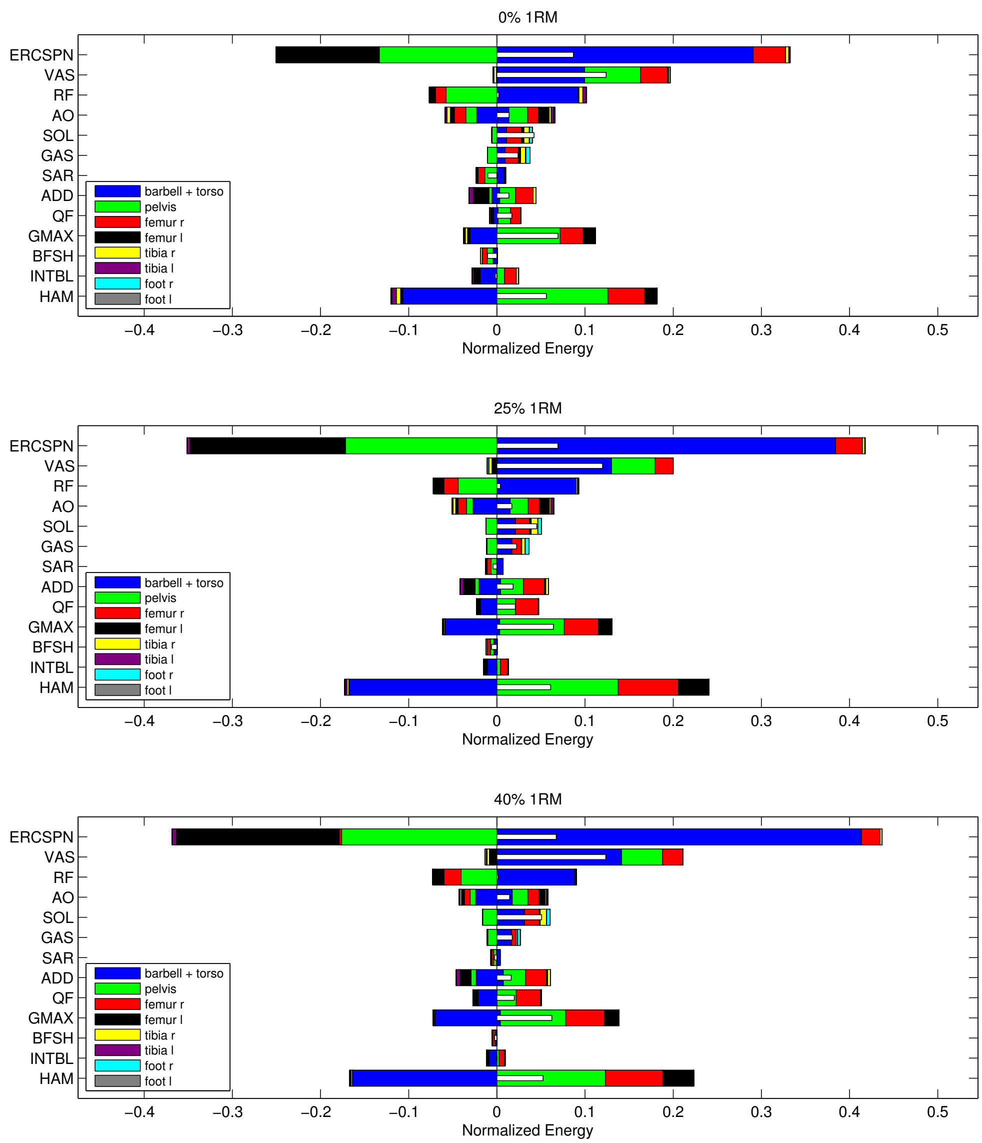

Figure 3.1: The flow of energy into and out of body segments from the action of muscles during the upward propulsive phase of the squat jump across a range of masses in the male athletes. The energy was normalized with the total energy produced during the propulsive phase of the jump. Positive values represent the contribution of energy to a segment, while negative values represent the withdrawal of energy from a segment. The white bars represent the work done by each muscle.

GMAX assisted HAM in the extension of the hip joint, and also increased the energy of the pelvis. However, this action also flexed the lumbar joint, and decreased the energy of the torso. While this action extended the knee joint, it also dorsiflexed the ankle joint. Along with ERCSPN, RF countered the actions of HAM and GMAX and extended the lumbar joint, thereby increasing the energy of the torso. However, this action flexed the hip joint, and decreased the energy of the pelvis. ERCSPN and RF functioned antagonistically to HAM and GMAX in relation to their actions on the pelvis and torso segments and at the lumbar and hip joints. Unlike VAS, SOL, and GMAX, these muscle groups transferred far more energy than they generated through contraction.

The primary role of VAS was to extend the knee joint and hip joint, and to contribute energy to both the torso and pelvis. This action caused a favorable extension of the hip joint, while having a minimal effect on the flexion of the lumbar joint. VAS caused slight dorsiflexion of the ankle joint. The dorsiflexion of the ankle joint by HAM, GMAX, and VAS was countered primarily by the plantar flexion by SOL and GAS. However, while this action caused a slight extension of the lumbar joint, it also caused flexion of the knee and hip joints. SOL and GAS primarily contributed energy to the ipsilateral femur and the torso and withdrew energy from the pelvis.

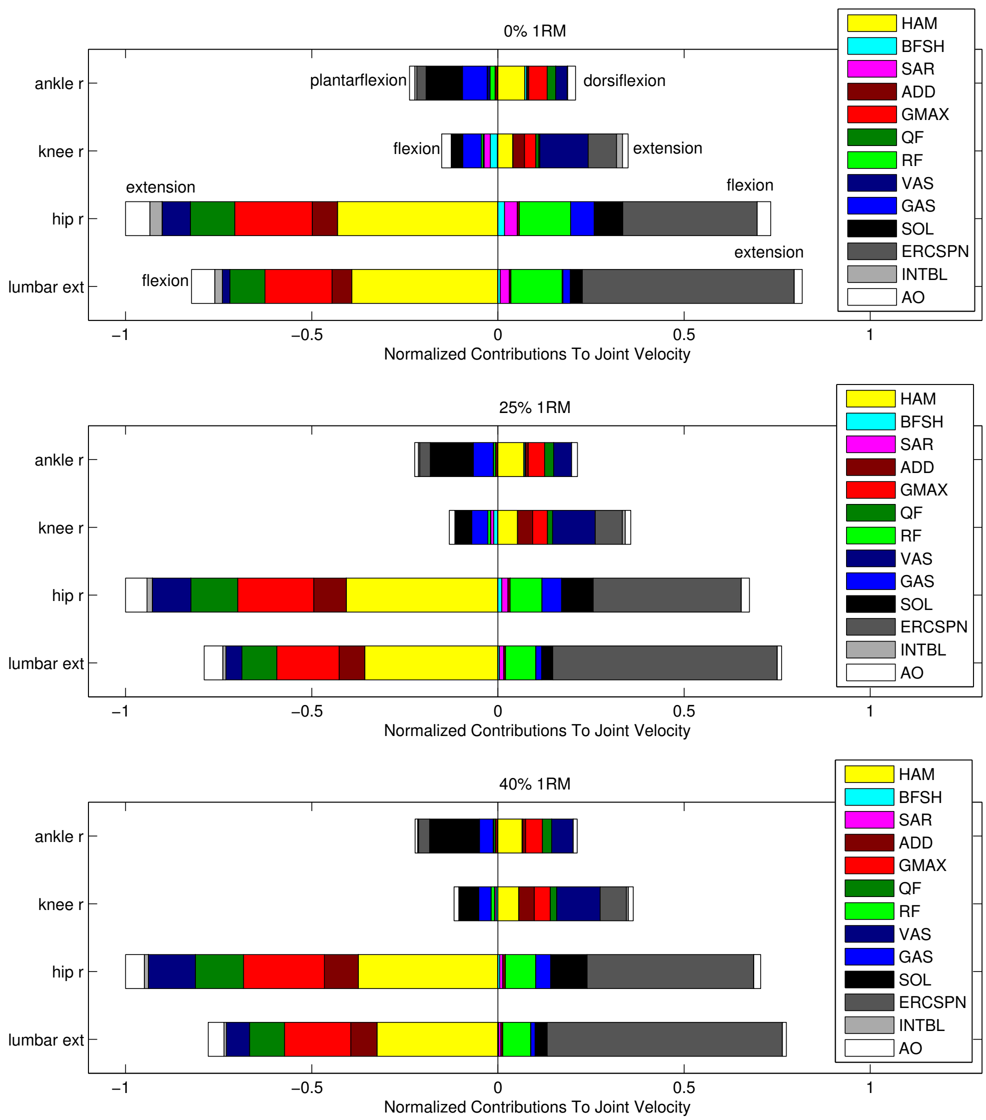

Figure 3.2: Joint accelerations induced by the action of muscles in the male athletes across a range of barbell masses. The joint accelerations were normalized according to the maximum absolute acceleration of each trial. Positive acceleration of the ankle, knee, hip, and lumbar joints represented dorsiflexion, extension, flexion, and extension respectively.

ADD and QF functioned similarly to GMAX and HAM by extending the hip joint, flexing the back joint, withdrawing energy from the torso, and contributing energy to the pelvis. SAR and BFSH did not have substantial contributions to either the energy of the segments or the acceleration of the joints.

Analysis of the energetic character of muscles revealed that ERCSPN, RF, HAM, and GMAX were primarily involved in transferring energy among segments, while VAS, SOL, and GAS primarily contributed positive energy to the body segments. VAS, SOL, and GAS did positive work as they contributed energy to segments, while RF did very little work despite transferring a great deal of energy.

3.1.2 Energetic changes across the range of barbell masses

The energy flow between muscles and body segments changed significantly between the loaded and unloaded squat jump conditions (Table 3.1). However, few differences in the flow of energy were present between the 25-40% 1RM barbell masses. Between the 0-40% 1RM masses, GMAX, HAM, QF, and ADD withdrew more energy from the torso, while SOL and VAS increased their contributions of energy to the torso. VAS decreased the positive energy it contributed to the pelvis with increasing masses while ERCSPN and SOL increased the withdrawal of energy from the pelvis.

There were significant differences between the induced joint accelerations across the range of barbell masses between the loaded and unloaded

Muscle and segment	0 and 25	0 and 40	25 and 40	0 - mean (s.d.)	25 - mean (s.d.)	40 - mean (s.d.)	0 and 40 difference
QF and barbell + torso	Yes	Yes	-	-0.004 (0.0036)	-0.0188 (0.0078)	-0.0215 (0.0064)	-0.0175
ADD and barbell + torso	Yes	Yes	-	-0.0057 (0.0035)	-0.0203 (0.0062)	-0.0235 (0.0082)	-0.0178
VAS and barbell + torso	Yes	Yes	-	0.0995 (0.0202)	0.1299 (0.0188)	0.1413 (0.0144)	0.0418
SOL and barbell + torso	Yes	Yes	Yes	0.011 (0.0046)	0.021 (0.0041)	0.0313 (0.0073)	0.0203
HAM and barbell + torso	Yes	Yes	-	-0.1069 (0.0301)	-0.168 (0.0475)	-0.164 (0.0526)	-0.0571
GMAX and barbell + torso	-	Yes	-	-0.0307 (0.0238)	-0.0591 (0.0233)	-0.0705 (0.026)	-0.0398
							-0.0701
VAS and pelvis	Yes	Yes	-	0.0636 (0.0076)	0.0494 (0.0084)	0.0466 (0.0148)	-0.017
ERCSPN and pelvis	-	Yes	-	-0.1335 (0.0203)	-0.1718 (0.0373)	-0.1761 (0.0406)	-0.0426
SAR and pelvis	Yes	Yes	-	-0.0138 (0.0061)	-0.0063 (0.0026)	-0.0032 (0.0027)	0.0106
BFSH and pelvis	Yes	Yes	Yes	-0.0065 (0.002)	-0.0037 (0.0017)	-0.0016 (0.0011)	0.0049
SOL and pelvis	Yes	Yes	-	-0.0057 (0.0037)	-0.0124 (0.0032)	-0.0161 (0.0058)	-0.0104
							-0.0545
QF and femur r	Yes	Yes	-	0.0114 (0.0057)	0.0252 (0.0095)	0.0279 (0.0126)	0.0165
INTBL and femur r	-	Yes	-	0.0135 (0.0076)	0.0074 (0.0049)	0.0056 (0.0044)	-0.0079
HAM and femur r	Yes	Yes	-	0.0418 (0.0128)	0.0683 (0.0168)	0.0652 (0.0108)	0.0234
GMAX and femur r	Yes	Yes	-	0.0262 (0.0104)	0.0388 (0.01)	0.0441 (0.0101)	0.0179
GAS and femur r	Yes	Yes	Yes	0.0153 (0.0047)	0.0103 (0.0039)	0.0051 (0.0031)	-0.0102
SAR and femur r	Yes	Yes	-	-0.0076 (0.0027)	-0.0045 (0.0023)	-0.0022 (0.0015)	0.0054
BFSH and femur r	-	Yes	-	-0.0055 (0.0025)	-0.0037 (0.0017)	-0.0017 (0.0009)	0.0038
							0.0489
AO and femur l	Yes	-	-	0.0169 (0.0088)	0.0084 (0.0054)	0.0105 (0.0061)	-0.0064
HAM and femur l	Yes	Yes	-	0.014 (0.0106)	0.0339 (0.0131)	0.0339 (0.0117)	0.0199
ERCSPN and femur l	Yes	Yes	-	-0.1162 (0.0302)	-0.1763 (0.0414)	-0.1845 (0.0465)	-0.0683
INTBL and femur l	Yes	Yes	-	-0.0072 (0.0042)	-0.0034 (0.0021)	-0.0024 (0.002)	0.0048
							0.05

Table 3.1: Significant differences in the energy flows by muscles on segments ($p<0.01$) between 0% 1RM, 25% 1RM, and 40% 1RM masses.

conditions (Table 3.2). Only one significant difference was present between the 25-40% 1RM barbell masses. With increased loading, the rate of lumbar extension decreased, the rate of hip and knee extension increased, and the rate of ankle plantar flexion decreased.

Muscle and joint	0 and 25	0 and 40	25 and 40	0 - mean (s.d.)	25 - mean (s.d.)	40 - mean (s.d.)	0 and 40 difference
RF and lumbar ext	Yes	Yes	-	0.1373 (0.0443)	0.0817 (0.0285)	0.0755 (0.0486)	-0.0618
SAR and lumbar ext	Yes	Yes	-	0.0245 (0.0117)	0.0118 (0.006)	0.0063 (0.0053)	-0.0182
GAS and lumbar ext	Yes	Yes	-	0.0199 (0.0039)	0.015 (0.0026)	0.0114 (0.0032)	-0.0085
BFSH and lumbar ext	Yes	Yes	-	0.0061 (0.0021)	0.0038 (0.002)	0.0017 (0.0013)	-0.0044
HAM and lumbar ext	-	Yes	-	-0.3923 (0.0401)	-0.3577 (0.0438)	-0.3249 (0.0522)	0.0674
INTBL and lumbar ext	Yes	Yes	-	-0.0203 (0.0129)	-0.0084 (0.0047)	-0.0066 (0.0045)	0.0137
VAS and lumbar ext	-	Yes	-	-0.0201 (0.0164)	-0.0432 (0.0172)	-0.062 (0.03)	-0.0419
							-0.0537
VAS and hip r	-	Yes	-	-0.0761 (0.0369)	-0.1033 (0.031)	-0.1262 (0.0444)	-0.0501
HAM and hip r	-	Yes	-	-0.431 (0.0302)	-0.4071 (0.0392)	-0.3749 (0.0504)	0.0561
INTBL and hip r	Yes	Yes	-	-0.0326 (0.0208)	-0.0142 (0.008)	-0.0108 (0.0073)	0.0218
BFSH and hip r	Yes	Yes	-	0.0179 (0.0064)	0.0104 (0.0057)	0.0045 (0.0037)	-0.0134
GAS and hip r	-	Yes	Yes	0.0632 (0.0132)	0.0523 (0.0059)	0.04 (0.0103)	-0.0232
SAR and hip r	Yes	Yes	-	0.034 (0.0137)	0.0164 (0.008)	0.0084 (0.0064)	-0.0256
RF and hip r	Yes	Yes	-	0.1377 (0.0406)	0.0856 (0.0312)	0.0816 (0.0541)	-0.0561
							-0.0905
GMAX and knee r	-	Yes	-	0.03 (0.0122)	0.0399 (0.0103)	0.043 (0.007)	0.013
QF and knee r	Yes	Yes	-	0.0085 (0.0035)	0.0138 (0.0049)	0.0173 (0.0038)	0.0088
INTBL and knee r	Yes	Yes	-	0.0161 (0.0097)	0.0076 (0.0048)	0.0052 (0.004)	-0.0109
BFSH and knee r	Yes	Yes	-	-0.0192 (0.0073)	-0.0108 (0.006)	-0.0046 (0.0041)	0.0146
GAS and knee r	-	Yes	-	-0.0493 (0.0114)	-0.0432 (0.005)	-0.033 (0.0095)	0.0163
SAR and knee r	Yes	Yes	-	-0.0168 (0.0059)	-0.008 (0.0037)	-0.0036 (0.0022)	0.0132
							0.055
GAS and ankle r	-	Yes	-	-0.0662 (0.0251)	-0.0535 (0.0137)	-0.0369 (0.0114)	0.0293
RF and ankle r	Yes	Yes	-	-0.0134 (0.0068)	-0.0051 (0.0038)	-0.0038 (0.0041)	0.0096
							0.0389

Table 3.2: Significant differences in the induced accelerations by muscles on joints ($p<0.01$) between 0% 1RM, 25% 1RM, and 40% 1RM masses.

3.2 Female athletes

3.2.1 Contributions of muscles to segmental energetics during the body-weight squat jump

The fundamental functional roles of the muscles in the women were nearly identical to those of the men (Figure 3.3). The primary difference in muscle function was the eccentric work done by RF in women compared to concentric work done in men. Induced joint accelerations also had the same fundamental patterns as the men (Figure 3.4). Statistical analysis between the men and women is shown in Section 3.3.

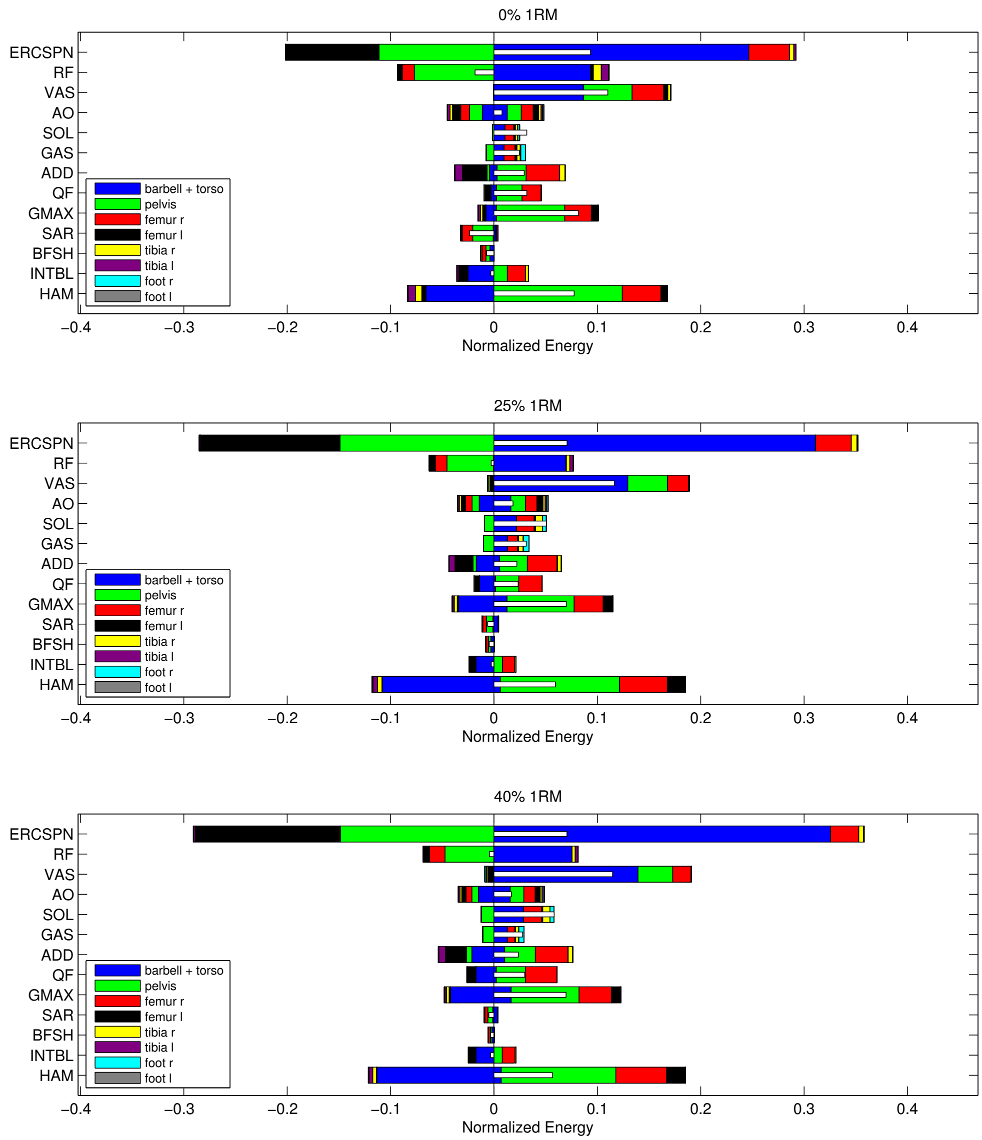

Figure 3.3: The flow of energy into and out of body segments from the action of muscles during the upward propulsive phase of the squat jump across a range of masses in the female athletes. The energy was normalized with the total energy produced during the propulsive phase of the jump. Positive values represent the contribution of energy to a segment, while negative values represent the withdrawal of energy from a segment. The white bars represent the work done by the muscle.

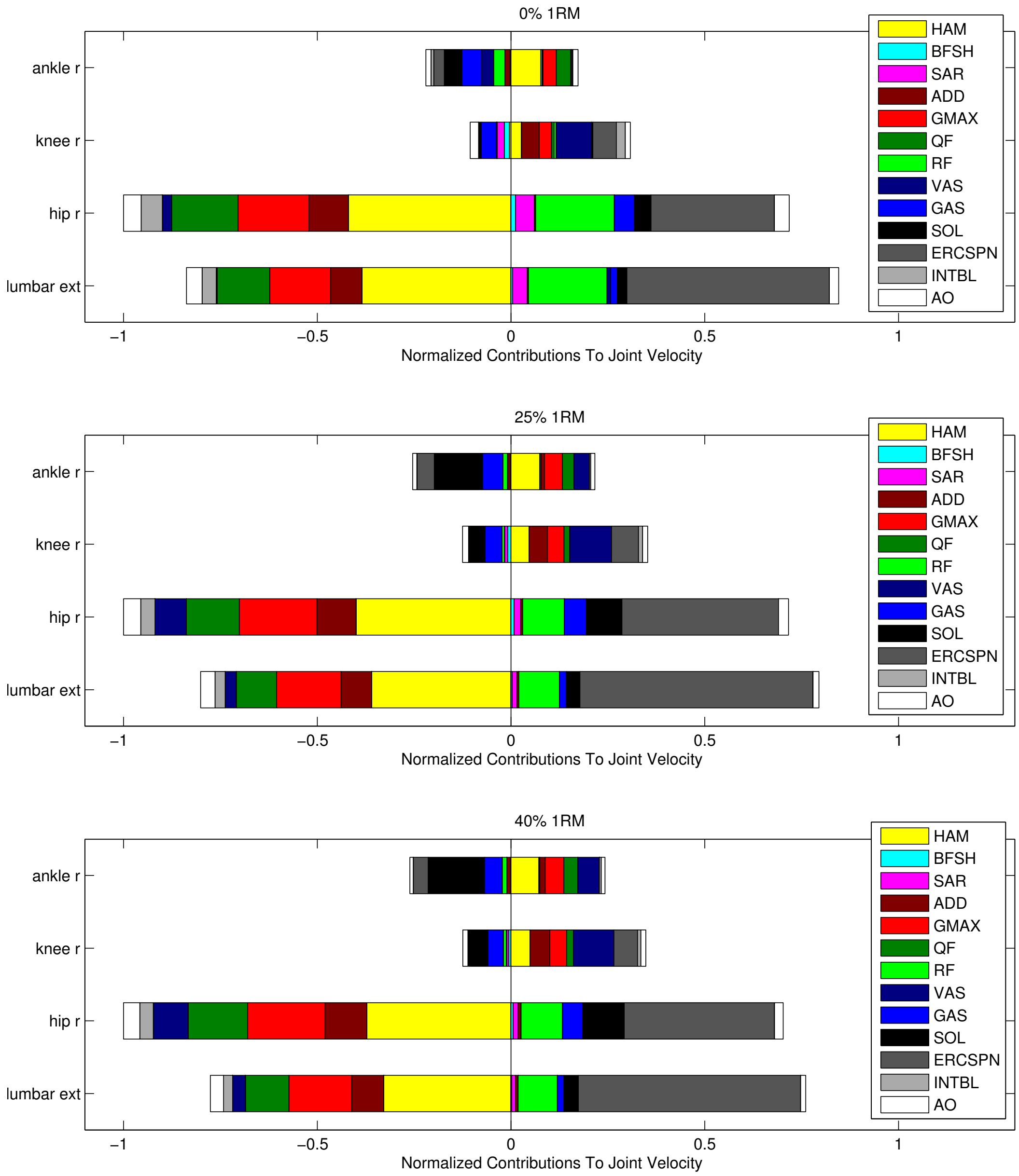

Figure 3.4: Joint accelerations induced by the action of muscles in the female athletes across a range of barbell masses. The joint accelerations were normalized according to the maximum absolute acceleration of each trial. Positive acceleration of the ankle, knee, hip, and lumbar joints represented dorsiflexion, extension, flexion, and extension respectively.

3.2.2 Energetic changes across the range of barbell masses

As was found with the male athletes, there were few significant differences in the transfer of energy between the 25-40% 1RM barbell masses (Table 3.3). When considering the unloaded and loaded conditions however, ERCSPN, VAS, and SOL increased their contributions of energy to the torso, while HAM and GMAX increased their withdrawal of energy from the torso resulting in a net increase in energy of the torso. RF, and GAS decreased their withdrawal of energy from the pelvis, while VAS decreased its positive contribution of energy to the pelvis resulting in a net decrease of energy in the pelvis.

Muscle and segment	0 and 25	0 and 40	25 and 40	0 - mean (s.d.)	25 - mean (s.d.)	40 - mean (s.d.)	0 and 40 difference
ERCSPN and barbell + torso	-	Yes	-	0.2465 (0.026)	0.3113 (0.0677)	0.3256 (0.0873)	0.0791
VAS and barbell + torso	Yes	Yes	-	0.0868 (0.0153)	0.1295 (0.0203)	0.1393 (0.0268)	0.0525
SOL and barbell + torso	Yes	Yes	Yes	0.0107 (0.0027)	0.0219 (0.005)	0.0286 (0.0082)	0.0179
ADD and barbell + torso	-	Yes	-	0.003 (0.0032)	0.0056 (0.0054)	0.0105 (0.0072)	0.0075
GMAX and barbell + torso	Yes	Yes	-	0.0025 (0.0047)	0.0127 (0.0105)	0.0166 (0.0125)	0.0141
BFSH and barbell + torso	-	Yes	-	-0.0039 (0.0017)	-0.0031 (0.0013)	-0.002 (0.0011)	0.0019
HAM and barbell + torso	Yes	Yes	-	-0.0658 (0.0275)	-0.1081 (0.0229)	-0.1133 (0.0285)	-0.0475
QF and barbell + torso	Yes	Yes	-	-0.0028 (0.0033)	-0.0139 (0.0066)	-0.0174 (0.0073)	-0.0146
ADD and barbell + torso	Yes	Yes	-	-0.0043 (0.0047)	-0.0171 (0.0069)	-0.0214 (0.0074)	-0.0171
GMAX and barbell + torso	Yes	Yes	-	-0.0077 (0.007)	-0.0345 (0.0081)	-0.0422 (0.0095)	-0.0345
							0.0593
RF and pelvis	Yes	Yes	-	-0.077 (0.0268)	-0.0449 (0.018)	-0.0472 (0.0254)	0.0298
SAR and pelvis	Yes	Yes	-	-0.0198 (0.0139)	-0.0062 (0.0046)	-0.0049 (0.0042)	0.0149
BFSH and pelvis	Yes	Yes	-	-0.0038 (0.0016)	-0.0022 (0.0012)	-0.0014 (0.0008)	0.0024
SOL and pelvis	Yes	Yes	Yes	-0.0013 (0.0016)	-0.0092 (0.0026)	-0.0123 (0.0027)	-0.011
ERCSPN and pelvis	Yes	Yes	-	-0.1113 (0.0177)	-0.149 (0.0338)	-0.1486 (0.0357)	-0.0373
VAS and pelvis	Yes	Yes	-	0.0468 (0.0068)	0.0384 (0.0071)	0.0336 (0.0064)	-0.0132
GAS and pelvis	Yes	Yes	-	-0.0073 (0.0027)	-0.01 (0.0014)	-0.0108 (0.0022)	-0.0035
							-0.0179
SAR and femur r	Yes	Yes	-	-0.0101 (0.0084)	-0.0035 (0.0029)	-0.0028 (0.0024)	0.0073
SOL and femur r	Yes	Yes	-	0.0084 (0.0044)	0.0169 (0.0046)	0.0173 (0.0062)	0.0089
HAM and femur r	-	Yes	-	0.0372 (0.0092)	0.0462 (0.0113)	0.0492 (0.0111)	0.012
QF and femur r	-	Yes	-	0.0185 (0.0083)	0.0223 (0.0077)	0.0304 (0.0167)	0.0119
BFSH and femur r	-	Yes	-	-0.0036 (0.0019)	-0.0023 (0.0012)	-0.0018 (0.0012)	0.0018
VAS and femur r	Yes	Yes	-	0.0306 (0.0085)	0.0204 (0.0073)	0.0177 (0.0074)	-0.0129
							0.029
HAM and femur l	Yes	Yes	-	0.0063 (0.0075)	0.0175 (0.0092)	0.0179 (0.0096)	0.0116
VAS and femur l	Yes	Yes	-	0.004 (0.0021)	0 (0.0002)	0 (0.0001)	-0.004
ERCSPN and femur l	Yes	Yes	-	-0.0903 (0.0195)	-0.1349 (0.0302)	-0.1395 (0.0328)	-0.0492
							-0.0416
HAM and tibia r	-	Yes	-	-0.006 (0.0021)	-0.0044 (0.0014)	-0.0036 (0.0015)	0.0024
RF and tibia r	Yes	Yes	-	0.0076 (0.0034)	0.0033 (0.0015)	0.003 (0.0019)	-0.0046
RF and tibia l	Yes	Yes	-	0.0072 (0.0031)	0.0033 (0.0016)	0.0027 (0.0016)	-0.0045
HAM and tibia l	Yes	Yes	-	-0.007 (0.0032)	-0.0042 (0.0018)	-0.0035 (0.0017)	0.0035
							-0.0032

Table 3.3: Significant differences ($p<0.01$) in the flow of energy between muscles and body segments across a range of barbell masses with the female athletes' squat jumps. Some muscle-segment groups may be listed twice because they represent the mean of the all the trials.

Similar to our findings with male athletes, the female athletes exhibited a reduced rate of lumbar extension, and increased rate of hip and knee extension with increased barbell masses (Table 3.4). Unlike the male athletes however, the female athletes increased the rate of ankle plantarflexion with increased barbell masses.

Muscle and joint	0 and 25	0 and 40	25 and 40	0 - mean (s.d.)	25 - mean (s.d.)	40 - mean (s.d.)	0 and 40 difference
SOL and lumbar ext	Yes	Yes	-	0.0246 (0.0047)	0.0347 (0.0081)	0.0373 (0.0088)	0.0127
BFSH and lumbar ext	-	Yes	-	0.0038 (0.0015)	0.0026 (0.0014)	0.0017 (0.001)	-0.0021
RF and lumbar ext	Yes	Yes	-	0.2029 (0.0531)	0.1046 (0.0449)	0.1014 (0.0527)	-0.1015
SAR and lumbar ext	Yes	Yes	-	0.0382 (0.028)	0.0128 (0.0082)	0.0098 (0.0073)	-0.0284
							-0.1193
VAS and hip r	Yes	Yes	-	-0.0239 (0.0138)	-0.0808 (0.0207)	-0.0902 (0.0303)	-0.0663
RF and hip r	Yes	Yes	-	0.2032 (0.048)	0.1075 (0.0444)	0.107 (0.0571)	-0.0962
SAR and hip r	Yes	Yes	-	0.0483 (0.0347)	0.0173 (0.0114)	0.0131 (0.0094)	-0.0352
BFSH and hip r	Yes	Yes	-	0.0116 (0.0047)	0.0078 (0.0039)	0.0052 (0.0028)	-0.0064
ERCSPN and hip r	Yes	-	-	0.3185 (0.0662)	0.4038 (0.072)	0.3879 (0.0834)	0.0694
SOL and hip r	Yes	Yes	-	0.0426 (0.016)	0.092 (0.0218)	0.1067 (0.0254)	0.0641
							-0.0706
GMAX and knee r	Yes	Yes	-	0.0316 (0.0079)	0.0426 (0.0093)	0.0435 (0.0107)	0.0119
QF and knee r	Yes	Yes	-	0.0067 (0.0054)	0.0147 (0.0054)	0.0174 (0.0068)	0.0107
SAR and knee r	Yes	Yes	-	-0.0182 (0.0115)	-0.0078 (0.0054)	-0.0054 (0.0036)	0.0128
BFSH and knee r	Yes	Yes	-	-0.013 (0.005)	-0.0086 (0.0044)	-0.0057 (0.003)	0.0073
HAM and knee r	Yes	Yes	-	0.0269 (0.0139)	0.0465 (0.0122)	0.0489 (0.0169)	0.022
INTBL and knee r	Yes	Yes	-	0.023 (0.0081)	0.0109 (0.0064)	0.0085 (0.007)	-0.0145
SOL and knee r	Yes	Yes	-	-0.0067 (0.0104)	-0.0424 (0.013)	-0.0517 (0.019)	-0.045
							0.0052
SOL and ankle r	Yes	Yes	-	-0.0456 (0.0271)	-0.1246 (0.0384)	-0.1454 (0.0474)	-0.0998
RF and ankle r	Yes	Yes	-	-0.029 (0.0085)	-0.0118 (0.0065)	-0.012 (0.0091)	0.017
GMAX and ankle r	Yes	Yes	-	0.0343 (0.0071)	0.0463 (0.0068)	0.0479 (0.0089)	0.0136
							-0.0692

Table 3.4: Significant differences ($p<0.01$) in the induced joint accelerations by muscles across a range of barbell masses in the female athletes' squat jumps.

3.3 Differences in muscular strategy between male and female squat jumps

There were significant differences between the flow of energy among muscles and body segments across all barbell masses between men and women (Table 3.5). However, the only positive difference between the energy contributions to the torso between men and women was found with SAR. This positive contribution was minimal relative to the other values. HAM and GMAX both withdrew more energy from the torso in the men than women.

Positive				**Negative**			
Muscle and segment	**Men - mean (s.d.)**	**Women - mean (s.d.)**	**Difference**	**Muscle and segment**	**Men - mean (s.d.)**	**Women - mean (s.d.)**	**Difference**
VAS and pelvis	0.0636 (0.0076)	0.0468 (0.0068)	0.0168	HAM and barbell + torso	-0.1069 (0.0301)	-0.0658 (0.0275)	-0.0411
SOL and femur r	0.0168 (0.0078)	0.0084 (0.0044)	0.0084	ERCSPN and femur l	-0.1162 (0.0302)	-0.0903 (0.0195)	-0.0259
SAR and barbell + torso	0.0085 (0.0067)	0.0018 (0.0015)	0.0067	GMAX and barbell + torso	-0.0307 (0.0238)	-0.0077 (0.007)	-0.023
GMAX and femur l	0.013 (0.0043)	0.0063 (0.0034)	0.0067	ERCSPN and pelvis	-0.1335 (0.0203)	-0.1113 (0.0177)	-0.0222
SOL and tibia r	0.006 (0.0042)	0.0021 (0.0015)	0.0039	SOL and pelvis	-0.0057 (0.0037)	-0.0013 (0.0016)	-0.0044
ADD and tibia r	0.0032 (0.0015)	0.0053 (0.0015)	-0.0021	GAS and pelvis	-0.0107 (0.0024)	-0.0073 (0.0027)	-0.0034
VAS and femur l	0.0011 (0.0012)	0.004 (0.0021)	-0.0029	VAS and tibia r	-0.0028 (0.0035)	-0.0001 (0.0002)	-0.0027
RF and tibia r	0.0044 (0.0016)	0.0076 (0.0034)	-0.0032	BFSH and pelvis	-0.0065 (0.002)	-0.0038 (0.0016)	-0.0027
RF and tibia l	0.0038 (0.0018)	0.0072 (0.0031)	-0.0034	GMAX and tibia l	-0.0011 (0.0009)	-0.0021 (0.0007)	0.001
ADD and pelvis	0.018 (0.0058)	0.0282 (0.0057)	-0.0102	ADD and tibia l	-0.0049 (0.0017)	-0.0072 (0.0018)	0.0023
QF and pelvis	0.0143 (0.0085)	0.0246 (0.008)	-0.0103				
ADD and femur r	0.0198 (0.0062)	0.0323 (0.0049)	-0.0125				

Table 3.5: Statistical differences (p<0.01) between male and female energy flows from muscles and segments with the body-weight squat jump.

With the 25% 1RM barbell mass, GMAX contributed more energy to the torso in the women than in the men, while HAM withdrew more energy from the torso in the men than women (Table 3.6). Similarly, GMAX withdrew more energy from the torso in the men than women. VAS contributed more energy to the pelvis in the men than in the women.

Positive				**Negative**			
Muscle and segment	**Men - mean (s.d.)**	**Women - mean (s.d.)**	**Difference**	**Muscle and segment**	**Men - mean (s.d.)**	**Women - mean (s.d.)**	**Difference**
HAM and pelvis	0.1376 (0.0259)	0.1154 (0.0206)	0.0222	HAM and barbell + torso	-0.168 (0.0475)	-0.1081 (0.0229)	-0.0599
HAM and femur r	0.0683 (0.0168)	0.0462 (0.0113)	0.0221	ERCSPN and femur l	-0.1763 (0.0414)	-0.1349 (0.0302)	-0.0414
HAM and femur l	0.0339 (0.0131)	0.0175 (0.0092)	0.0164	GMAX and barbell + torso	-0.0591 (0.0233)	-0.0345 (0.0081)	-0.0246
VAS and pelvis	0.0494 (0.0084)	0.0384 (0.0071)	0.011	RES_ACT and femur l	-0.0173 (0.0088)	-0.0081 (0.0094)	-0.0092
GMAX and femur r	0.0388 (0.01)	0.0281 (0.0071)	0.0107	RF and femur l	-0.0117 (0.0071)	-0.006 (0.0046)	-0.0057
GMAX and femur l	0.0145 (0.0046)	0.009 (0.0037)	0.0055	SOL and pelvis	-0.0124 (0.0032)	-0.0092 (0.0026)	-0.0032
QF and tibia r	0.0008 (0.0005)	0.0002 (0.0003)	0.0006	ERCSPN and tibia l	-0.0033 (0.0017)	-0.0012 (0.0017)	-0.0021
RF and tibia r	0.0016 (0.0009)	0.0033 (0.0015)	-0.0017	BFSH and pelvis	-0.0037 (0.0017)	-0.0022 (0.0012)	-0.0015
RF and tibia l	0.0012 (0.0008)	0.0033 (0.0016)	-0.0021	BFSH and femur r	-0.0037 (0.0017)	-0.0023 (0.0012)	-0.0014
ERCSPN and tibia r	0.0025 (0.0022)	0.0054 (0.0025)	-0.0029	SAR and tibia r	-0.0009 (0.0007)	-0.0003 (0.0003)	-0.0006
GMAX and barbell + torso	0.0032 (0.0038)	0.0127 (0.0105)	-0.0095	BFSH and tibia r	-0.0012 (0.0007)	-0.0006 (0.0004)	-0.0006
				QF and tibia r	0 (0)	-0.0005 (0.0005)	0.0005
				GMAX and tibia l	-0.0005 (0.0005)	-0.0014 (0.0006)	0.0009
				GMAX and tibia r	-0.0013 (0.001)	-0.0029 (0.0005)	0.0016
				HAM and tibia r	-0.002 (0.0017)	-0.0044 (0.0014)	0.0024
				HAM and tibia l	-0.0017 (0.0014)	-0.0042 (0.0018)	0.0025

Table 3.6: Statistical differences (p<0.01) between male and female energy flows from muscles and segments with the 25% 1RM squat jump.

With the 40% 1RM barbell mass, GMAX again contributed more energy to the torso in the women compared to men (Table 3.7). HAM and GMAX also withdrew more energy from the torso in the men than women, while VAS contributed more energy to the pelvis in men than in the women.

Positive				**Negative**			
Muscle and segment	**Men - mean (s.d.)**	**Women - mean (s.d.)**	**Difference**	**Muscle and segment**	**Men - mean (s.d.)**	**Women - mean (s.d.)**	**Difference**
HAM and femur l	0.0339 (0.0117)	0.0179 (0.0096)	0.016	HAM and barbell + torso	-0.164 (0.0526)	-0.1133 (0.0285)	-0.0507
HAM and femur r	0.0652 (0.0108)	0.0492 (0.0111)	0.016	ERCSPN and femur l	-0.1845 (0.0465)	-0.1395 (0.0328)	-0.045
VAS and pelvis	0.0466 (0.0148)	0.0336 (0.0064)	0.013	GMAX and barbell + torso	-0.0705 (0.026)	-0.0422 (0.0095)	-0.0283
GMAX and femur r	0.0441 (0.0101)	0.0315 (0.0099)	0.0126	ERCSPN and tibia l	-0.0049 (0.0034)	-0.0017 (0.0024)	-0.0032
GMAX and femur l	0.0156 (0.0051)	0.0085 (0.0042)	0.0071	ADD and femur r	-0.0006 (0.0005)	-0.0001 (0.0005)	-0.0005
QF and tibia r	0.0008 (0.0007)	0.0002 (0.0004)	0.0006	GAS and tibia l	-0.0001 (0.0001)	0 (0)	-0.0001
HAM and tibia r	0.0007 (0.0009)	0.0001 (0.0002)	0.0006	QF and tibia r	0 (0.0001)	-0.0004 (0.0004)	0.0004
GAS and tibia r	0.0013 (0.0013)	0.0031 (0.0015)	-0.0018	GMAX and tibia l	-0.0004 (0.0004)	-0.0014 (0.0007)	0.001
RF and tibia l	0.0008 (0.0008)	0.0027 (0.0016)	-0.0019	GMAX and tibia r	-0.0009 (0.001)	-0.0026 (0.0008)	0.0017
RF and tibia r	0.001 (0.0009)	0.003 (0.0019)	-0.002	HAM and tibia r	-0.0014 (0.002)	-0.0036 (0.0015)	0.0022
ERCSPN and tibia r	0.002 (0.0022)	0.0047 (0.0025)	-0.0027	HAM and tibia l	-0.0011 (0.0009)	-0.0035 (0.0017)	0.0024
GMAX and barbell + torso	0.0039 (0.0055)	0.0166 (0.0125)	-0.0127	ADD and femur l	-0.0119 (0.0037)	-0.0201 (0.0102)	0.0082

Table 3.7: Statistical differences (p<0.01) between male and female energy flows from muscles and segments with the 40% 1RM squat jump.

Statistical analysis of the induced joint accelerations showed 26 differences between the men and women occurred at the body-weight squat jump (Table 3.8). Six differences occurred at each of the 25% 1RM and 40% 1RM masses. Eight of the 26 differences at the body-weight squat jump involved changes in the lumbar joint motion, seven differences involved the hip joint, and five differences involved the knee joint.

0% 1 RM - Positive				**0% 1 RM - Negative**			
Muscle and joint	**Men - mean (s.d.)**	**Women - mean (s.d.)**	**Difference**	**Muscle and joint**	**Men - mean (s.d.)**	**Women - mean (s.d.)**	**Difference**
VAS and knee r	0.1298 (0.0218)	0.0919 (0.0205)	0.0379	SOL and ankle r	-0.098 (0.0466)	-0.0456 (0.0271)	-0.0524
SOL and hip r	0.077 (0.0331)	0.0426 (0.016)	0.0344	VAS and hip r	-0.0761 (0.0369)	-0.0239 (0.0138)	-0.0522
VAS and ankle r	0.0313 (0.0356)	0.0014 (0.0059)	0.0299	SOL and knee r	-0.0312 (0.0186)	-0.0067 (0.0104)	-0.0245
ERCSPN and knee r	0.0762 (0.0147)	0.0606 (0.0105)	0.0156	GMAX and lumbar ext	-0.18 (0.0204)	-0.1569 (0.0208)	-0.0231
GMAX and ankle r	0.0497 (0.0115)	0.0343 (0.0071)	0.0154	VAS and lumbar ext	-0.0201 (0.0164)	-0.0022 (0.0047)	-0.0179
BFSH and hip r	0.0179 (0.0064)	0.0116 (0.0047)	0.0063	BFSH and knee r	-0.0192 (0.0073)	-0.013 (0.005)	-0.0062
BFSH and lumbar ext	0.0061 (0.0021)	0.0038 (0.0015)	0.0023	RF and ankle r	-0.0134 (0.0068)	-0.029 (0.0085)	0.0156
VAS and lumbar ext	0.0023 (0.0052)	0.0094 (0.0071)	-0.0071	INTBL and lumbar ext	-0.0203 (0.0129)	-0.0363 (0.0146)	0.016
QF and ankle r	0.0231 (0.0107)	0.0377 (0.0073)	-0.0146	INTBL and hip r	-0.0326 (0.0208)	-0.0546 (0.0197)	0.022
ADD and knee r	0.0311 (0.0063)	0.046 (0.0126)	-0.0149	VAS and ankle r	-0.0077 (0.0164)	-0.0307 (0.0179)	0.023
RF and hip r	0.1377 (0.0406)	0.2032 (0.048)	-0.0655	ADD and lumbar ext	-0.0531 (0.0167)	-0.0807 (0.0194)	0.0276
RF and lumbar ext	0.1373 (0.0443)	0.2029 (0.0531)	-0.0656	ADD and hip r	-0.0675 (0.0163)	-0.102 (0.0208)	0.0345
				QF and lumbar ext	-0.0946 (0.0489)	-0.1361 (0.0322)	0.0415
				QF and hip r	-0.119 (0.0522)	-0.1715 (0.0303)	0.0525
25% 1 RM - Positive				**25% 1 RM - Negative**			
Muscle and joint	**Men - mean (s.d.)**	**Women - mean (s.d.)**	**Difference**	**Muscle and joint**	**Men - mean (s.d.)**	**Women - mean (s.d.)**	**Difference**
GAS and lumbar ext	0.015 (0.0026)	0.0182 (0.0032)	-0.0032	ERCSPN and ankle r	-0.0288 (0.0135)	-0.0448 (0.0158)	0.016
				INTBL and hip r	-0.0142 (0.008)	-0.0369 (0.0271)	0.0227
				INTBL and lumbar ext	-0.0084 (0.0047)	-0.0262 (0.0219)	0.0178
				RF and ankle r	-0.0051 (0.0038)	-0.0118 (0.0065)	0.0067
				INTBL and ankle r	-0.0033 (0.0023)	-0.0004 (0.0006)	-0.0029
40% 1 RM - Positive				**40% 1 RM - Negative**			
Muscle and joint	**Men - mean (s.d.)**	**Women - mean (s.d.)**	**Difference**	**Muscle and joint**	**Men - mean (s.d.)**	**Women - mean (s.d.)**	**Difference**
GAS and hip r	0.04 (0.0103)	0.0525 (0.0094)	-0.0125	VAS and hip r	-0.1262 (0.0444)	-0.0902 (0.0303)	-0.036
GAS and lumbar ext	0.0114 (0.0032)	0.0168 (0.0037)	-0.0054	VAS and lumbar ext	-0.062 (0.03)	-0.033 (0.0174)	-0.029
				RF and ankle r	-0.0038 (0.0041)	-0.012 (0.0091)	0.0082
				INTBL and ankle r	-0.0021 (0.0023)	-0.0003 (0.0008)	-0.0018

Table 3.8: Statistical differences (p<0.01) between male and female induced accelerations with the 0, 25, and 40% 1RM squat jumps.

3.4 Model validation

The mean intensity profiles for experimental EMG data and muscle forces calculated via static optimization compared reasonably well with one another across different masses and genders (Figure 3.5). Both EMG and force data for RF showed a peak just prior to lift-off. However, EMG data for RF showed more activity during the earlier phase of the squat jump. The estimated forces in vastus lateralis (VL) peaked earlier and were broader than the EMG data for VL. GMAX profiles for the EMG force data compared well for nearly all masses for both men and women. However, the men's GMAX EMG profile for the 40% 1RM mass peaked earlier, and was broader than the EMG profile.

The total energy generated during the squat jump was calculated with several different methods (Figure 3.6): 1) The integral of the power calculated by multiplying the total vertical ground reaction force with the velocity of the center of mass, 2) The sum of the kinetic and potential energy of all the segments 3) The total energy calculated with the Pseudo-Inverse Induced Acceleration Analysis (PIAA) plug-in with the contributions from the actuators, gravity, and velocity (AGV), 4) The total energy calculated with the PIAA plug-in showing only the contributions from the muscles, 5) The total energy generated from the muscles and the residual and reserve actuators, and 6) The total energy generated by only the muscles.

There was excellent agreement between energy calculated via the experimental methods and the PIAA plug-in. However, the energy calculated via

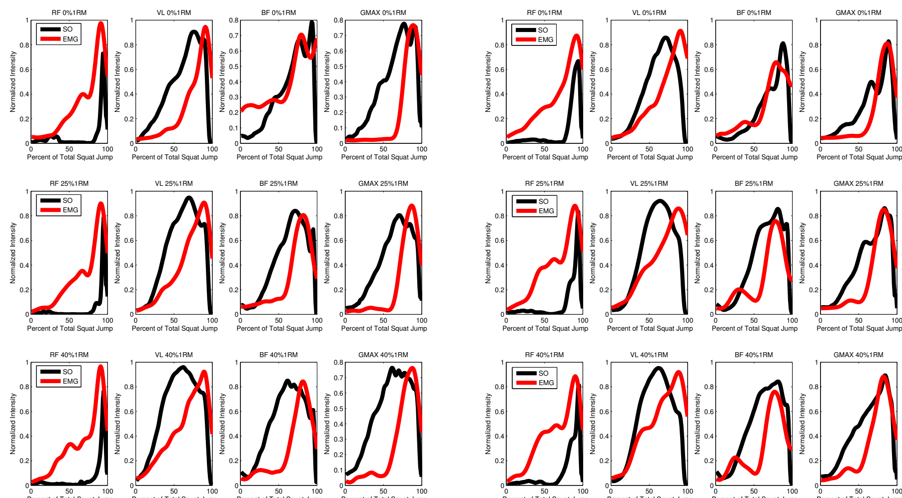

(a) (b)

Figure 3.5: The mean EMG intensity (red) and static optimization muscle forces (black) for RF, vastus lateralis (VL), biceps femoris (BF), and GMAX for the men and women were normalized with the maximum value of each trial. The period of time shown was from the initial upright standing position to lift-off. (a) Men; (b) Women

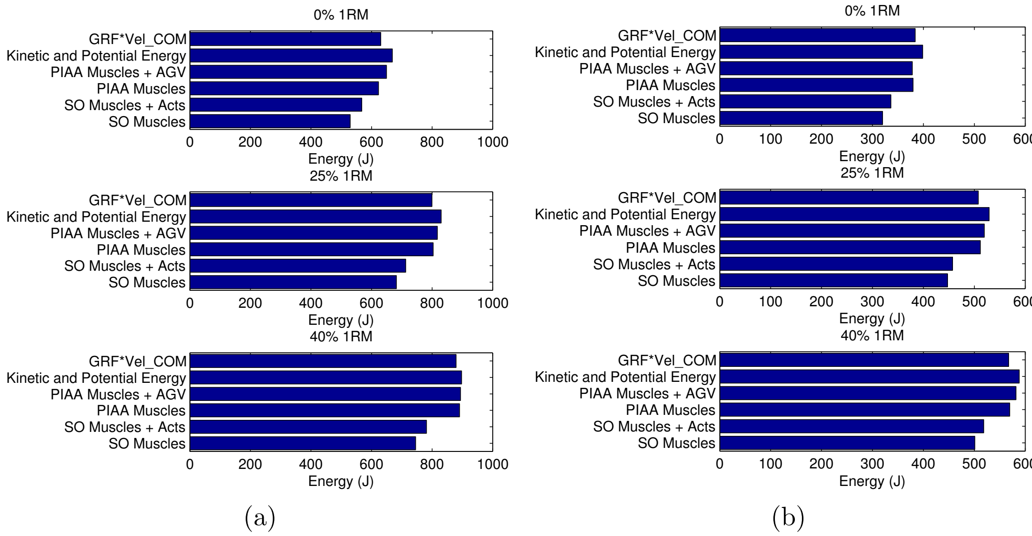

Figure 3.6: Different methods for calculating the energy generated during the upward propulsive phase of the squat jump were compared. These methods consisted of 1) The integral of the ground reaction force multiplied by the velocity of the center of mass, 2) The kinetic and potential energy of all the segments of the body 3) The energy calculated from the PIAA plug-in along with the contributions from the actuators, gravity, and velocity, 4) The energy calculated with the PIAA plug-in from the action of the muscles alone, 5) The energy calculated from work done by the muscles and the actuators, and 6) The energy calculated from the work done by the muscles only. (a) Men; (b) Women

the muscles forces and actuators was lower than the values obtained via the preceding methods, likely because static optimization neglects Coriolis and centripetal accelerations. Notably, it can be seen that the contributions of the residual and reserve actuators are minimal in both the PIAA plug-in and muscle energy methods indicating that nearly all the energy generated in the simulation is a result of the action of the muscles.

Chapter 4

Discussion

The goal of this study was to obtain a comprehensive understanding of the role of muscles in generating, absorbing, and transferring energy among the body segments during the squat jump. Our simulation results showed the individual energetic contributions of muscles to all segments of the body. This enabled us to identify, redefine, and clarify the functional role of muscles during the squat jump. We characterized the energetic character of muscles in introducing and transferring energy throughout the body. Finally, our results showed the differences between the coordination strategies that men and women use to support and propel increased barbell masses.

4.1 Coordination principles of the squat jump

Our results revealed whole-body coordination principles during the squat jump. Because the torso is the largest body segment, we focused on the coordination principles that led to the contribution of energy to the torso. Our simulation showed that the contraction of ERCSPN caused extension of the lumbar joint, and contributed energy to the torso. However, this contraction also caused unfavorable flexion of the hip joint. HAM was the primary muscle group that countered this flexion by acting to extend the hip joint. This action by HAM also flexed the lumbar joint and withdrew energy from the torso. HAM was assisted in its extension of the hip joint by GMAX and VAS. The action of ERCSPN and RF in extending the lumbar and hip joints was countered by the action of HAM, GMAX, and VAS muscles. This suggests that these muscles act synergistically to contribute positive net energy to the torso. This finding supports the results by Prilutsky & Zatsiorsky (1994) who reported that RF and HAM were involved in an antagonistic relationship in transferring joint energy to and from proximal and distal joints. Our results also support the findings by Pandy & Zajac (1991) who reported that GMAX and VAS acted together to cause hip and knee extension. However, our simulation showed that HAM and GMAX cause lumbar flexion and hip extension, while their model showed that HAM and GMAX cause lumbar extension. If we locked the lumbar joint on our model, hip extension would cause upward rotation of the torso, indicating that the differences between our studies are due to our inclusion of a lumbar joint.

VAS contributed the second most energy to the torso. While ERCSPN acted synergistically with HAM and GMAX to extend the lumbar and hip joint, VAS increased the energy of the torso by extending the knee joint. The extension of the knee joint resulted primarily in the translation of both the pelvis and the torso. The contribution of energy to both the pelvis and torso was a unique feature of VAS, as most other muscles are involved in a reciprocal energy relationship with the pelvis and torso. VAS was also unique among the muscles as its contraction resulted primarily in favorable joint rotations. Pandy & Zajac (1991) reported a similar function of VAS, likely because VAS does not primarily act to flex or extend the lumbar joint.

RF followed VAS and ERCSPN in the amount of energy contributed to the torso. Its mechanism of action was more complex than that of VAS and ERCSPN, likely due to its biarticular configuration. Our simulation showed that it primarily extended the lumbar joint and flexed the hip joint, thereby contributing energy to the torso and withdrawing energy from the pelvis and ipsilateral femur. This action is consistent with the hypothesis that RF is involved in the conversion of rotational kinetic energy into vertical translational kinetic energy (Van Ingen Schenau, 1989). In further support of this hypothesis, the EMG and force profiles reach peak intensity just prior to lift-off. Our findings contrast those reported by Pandy & Zajac (1991). Their simulation showed that RF had negligible contributions to joint rotations. However, this may be because their simulation differed from experimental results by exhibiting increasing segmental angular velocities at lift-off.

Our simulation results showed that SOL and GAS function in fundamentally the same manner. Both muscles plantarflexed the ankle joint, flexed the knee and hip joints, and extended the back joint. These results are consistent with those reported by Pandy & Zajac (1991). Some researchers have suggested that the biological rationale for biarticular plantar flexors is to increase the power output of the ankle joint (Gregoire *et al.*, 1984; Bobbert & van Ingen Schenau, 1988; van Soest *et al.*, 1993). Given that the energetic contributions of GAS decrease with larger barbell masses, and consequently, slower joint velocities, our results suggest that the biarticular nature of GAS may indeed be enhancing its ability to plantarflex the ankle joint during more rapid body-weight squat jumps.

4.2 Hypothesis 1: Biarticular muscles will transfer more energy than they generate.

Our results showed that biarticular RF and HAM transferred more energy among body segments than they generated through their contraction alone. However, GAS generated more energy than it transferred to the body segments, while SAR contracted eccentrically, and primarily absorbed energy from segments. Thus, not all biarticular muscles transferred more energy than they generated.

Analyzing the energetic character of muscles enabled us to obtain a greater understanding of the coordination principles of the squat jump. VAS, SOL, and GAS primarily contributed energy to the body segments, thus taking on the role of net energy generators in the body. These muscles did not have large antagonistic energetic relationships with other body segments, suggesting that these muscles primarily exerted forces on the ground to increase the translational kinetic energy of the body.

ERCSPN, RF, and HAM were heavily involved in transferring energy among body segments and also primarily caused rotation about the lumbar and hip joints. ERCSPN and HAM increased the rotational energy of the body during the early phase of the jump, while RF opposed rotation at the end of the jump. ERCSPN and HAM both expended much energy, which suggests they are active throughout much of the jump. RF did negligible work, indicating that it is active only for a short period of time at lift-off. These results suggest that ERCSPN, RF, and HAM are responsible for transferring rotational energy throughout the body.

In contrast to the more singular role of the preceding muscles, GMAX appears to increase both the rotational and translational energy of the body. This claim is supported by the fact that GMAX did a great deal of work during the jump and had a substantial positive net energy contribution to the body, yet still is involved in a reciprocal relationship between the pelvis and torso.

4.3 Hypothesis 2: Muscles redistribute their contributions over increasing barbell masses.

The majority of the energetic differences were found between the body-weight and loaded squat jumps, while few differences were found between the 25% and 40% 1RM squat jumps. The fundamental kinematic differences between the body-weight and loaded squat jumps were decreased lumbar extension, increased hip extension, increased knee extension, and decreased ankle plantarflexion in the loaded squat jump. These results are consistent from a dynamical perspective: A greater barbell mass will increase the torque at the lumbar joint, thus making it more difficult to increase the rate of extension. Similarly, the plantarflexors must now counteract a greater torque at the ankle joint. Consistent with these kinematic results, our simulations showed that the loaded condition resulted in less energy being transferred by the muscles to the torso and pelvis, and more energy transferred to the femur.

VAS and SOL increased their contributions of normalized energy to the torso with the loaded squat jump. Our analyses showed that VAS and SOL had few antagonistic relationships, and primarily contributed energy to the body. Accordingly, both of these muscles can generate more force to support the increased loads. Notably, GAS did not mirror SOL with increased contributions. This is likely because the biarticular configuration of GAS would cause it to flex the knee joint if it contracted during the lowest squat phase of the jump. GAS instead contracted late in the jump during ankle extension.

RF decreased its extension of the lumbar joint and flexion of the lumbar joint with increased barbell masses. This result supports the claim that RF converts rotational energy into translational energy. Because the larger masses result in reduced vertical jump velocities, squat jumps with higher masses will have less rotational and translational kinetic energy to convert into vertical translational kinetic energy.

Our results suggest that the body adopts a 'loaded' muscular strategy in response to increased loads, and maintains that strategy across a range of loads. Evaluating the functional role of muscles across a range of loads also served as a type of sensitivity analysis, and further supports our claims for the functional roles of the muscles.

4.4 Hypothesis 3: Men and women use different strategies to support and propel the increased barbell mass.

Our simulations showed that the fundamental functional role of the muscles of men and women remained the same across the range of barbell masses. This result is consistent with the fact that men and women exhibit the same general kinematic patterns during the squat jump. However, statistical analyses of the contributions of the muscles to joint accelerations and segmental energetics showed that there were many differences between the men's and women's body-weight squat jump strategies. Because women have a greater cross sectional area of fat in their bodies when compared to men (Kanehisa *et al.*, 1994), the unloaded condition may amplify the dynamical effects of this distribution. Adding a constraint on the body with the barbell may cause the men and women to converge on one optimized propulsive solution, thus reducing the dynamical effects of this distribution.

Insight into the differences in the function of individual muscles between men and women is limited because the same general musculoskeletal model was used for both men and women. While each segment was scaled individually, properties such as muscle composition, muscle routing patterns, and the orientation of skeletal segments with respect to one another were not altered. Considering these limitations, we will evaluate only the greatest changes in muscle function between men and women during the body-weight squat jump.

Our results showed that VAS contributes more energy to the pelvis in men than women, while SOL provides more energy to the femur. In men, VAS contributed more to hip and knee extension while SOL contributed more to ankle plantarflexion. However, RF contributed more to lumbar extension and hip flexion in women than men. These results suggest that the energy generating muscles are more active in men than women, while the energy transferring muscles more active in women than men. Given that men are stronger than women even after normalizing the strength with the fat-free mass of the individual (Frontera *et al.*, 1991), men may be able to adopt a jumping strategy that is only possible with a higher strength-to-mass ratio during the body-weight jumping condition.

We conclude that the fundamental squat jump strategies between men and women remain the same across the range of barbell masses. However, during the body-weight squat jump, our results suggest that men increase their use of muscles that increase the translational energy of the body, while women increase their use of muscles that transfer energy among body segments.

4.5 Modeling methodologies

We used static optimization to determine the muscle forces produced during the squat jump. In a comparison of static and dynamic optimization solutions for gait, Anderson & Pandy (2001) found that the solutions are 'practically equivalent'. Further, both static and dynamic optimization have been used to evaluate the function of muscles during running, and have yielded the same conclusions (Hamner *et al.*, 2010; Dorn *et al.*, 2012a). Because the joint angular velocities involved in the squat jump are comparable to those of running, we are confident with the use of static optimization in our study.

The comparisons of the intensity profiles for EMG and force data shows that some of the peaks align well with one another. While a delay of 81.9 ms between the EMG signal and the force production of the muscle has been reported with the vastus lateralis (Vos *et al.*, 1990), it would be difficult to discern a delay this small given the relative duration of the ground contact phase of the jump. While the force for RF spikes rapidly at the end of the jump, the EMG profiles increases to the peak more gradually. This may be because RF is functioning passively as a 'inextensible cord' at the end of the jump phase, and is being actively pulled taut by other muscles and motion of the body. The peaks for the intensity of VL become increasing shifted with increasing barbell masses. However, our force profiles for VL are consistent with the squat jump EMG intensity profiles for VL from other studies (Bosco *et al.*, 1982; Pandy & Zajac, 1991). EMG and force intensity profiles for GMAX were nearly the same for all the women, but became less similar for the men with greater barbell masses. The EMG force intensity profiles for BF were similar across all masses with men and women.

Incorporating experimental data into a musculoskeletal model introduces certain limitations. Markers placed on the athletes are subject to motion artifacts resulting from relative motion between the marker and the underlying skeleton. We accounted for this by weighting the markers we had more confidence in more heavily. While the human body has degrees of freedom between each vertebra, our model had a rigid torso unit. However, because we analyzed the fundamental whole body coordination principles, the limited motion at each vertebra is unlikely to have a substantial effect on the results. Insight into the coordination patterns between men and women was also limited because we scaled the same model for both genders. Because of this, we were conservative in our interpretation of the coordination differences between men and women.

Appendix

	barbell + torso	**pelvis**	**femur r**	**femur l**	**tibia r**	**tibia l**	**foot r**	**foot l**
HAM	0 (0)	0.1259 (0.0136)	0.0418 (0.0128)	0.014 (0.0106)	0 (0)	0 (0)	0 (0)	0 (0)
BFSH	0 (0)	0 (0)	0 (0)	0.0001 (0.0002)	0 (0)	0.0001 (0.0001)	0.0004 (0.0001)	0 (0)
SAR	0.0085 (0.0067)	0 (0)	0 (0)	0.0004 (0.0008)	0 (0)	0.0007 (0.0006)	0.0003 (0.0002)	0.0002 (0.0001)
ADD	0.0032 (0.0042)	0.018 (0.0058)	0.0198 (0.0062)	0.0002 (0.0004)	0.0032 (0.0015)	0 (0)	0.0001 (0.0001)	0 (0)
GMAX	0.0001 (0.0003)	0.0716 (0.0116)	0.0262 (0.0104)	0.013 (0.0043)	0.0001 (0.0003)	0.0009 (0.0006)	0 (0)	0.0001 (0.0001)
QF	0.0013 (0.0026)	0.0143 (0.0085)	0.0114 (0.0057)	0 (0.0001)	0.0002 (0.0003)	0.0001 (0.0001)	0 (0)	0 (0)
RF	0.0922 (0.026)	0 (0)	0.0003 (0.0011)	0.0006 (0.002)	0.0044 (0.0016)	0.0038 (0.0018)	0 (0)	0.0005 (0.0001)
VAS	0.0995 (0.0202)	0.0636 (0.0076)	0.0306 (0.0102)	0.0011 (0.0012)	0.0016 (0.002)	0.0002 (0.0002)	0 (0)	0.0001 (0)
GAS	0.0093 (0.006)	0 (0)	0.0153 (0.0047)	0.0024 (0.0014)	0.0054 (0.0044)	0.0006 (0.0002)	0.0047 (0.0017)	0 (0)
SOL	0.011 (0.0046)	0 (0)	0.0168 (0.0078)	0.0029 (0.002)	0.006 (0.0042)	0.0003 (0.0002)	0.0032 (0.0014)	0 (0)
ERCSPN	0.2906 (0.0716)	0 (0)	0.037 (0.0142)	0 (0)	0.0035 (0.0019)	0.0014 (0.0018)	0.0001 (0.0001)	0.0003 (0.0002)
INTBL	0 (0)	0.0086 (0.0058)	0.0135 (0.0076)	0 (0)	0.0024 (0.0016)	0 (0)	0.0003 (0.0003)	0 (0)
AO	0.0104 (0.0067)	0.0085 (0.0098)	0.0233 (0.0179)	0.0169 (0.0088)	0.0051 (0.0022)	0.005 (0.0017)	0.0014 (0.0003)	0.0014 (0.0004)

Table A.1: Men 0% 1RM: Normalized positive energy flows and standard deviation.

	barbell + torso	**pelvis**	**femur r**	**femur l**	**tibia r**	**tibia l**	**foot r**	**foot l**
HAM	-0.1069 (0.0301)	0 (0)	0 (0)	-0.0023 (0.0059)	-0.0049 (0.0025)	-0.0051 (0.0021)	-0.0008 (0.0004)	-0.0003 (0.0001)
BFSH	-0.0045 (0.0026)	-0.0065 (0.002)	-0.0055 (0.0025)	-0.0001 (0.0002)	-0.002 (0.0017)	0 (0)	0 (0)	0 (0)
SAR	0 (0)	-0.0138 (0.0061)	-0.0076 (0.0027)	-0.0007 (0.0009)	-0.0013 (0.0012)	0 (0.0001)	0 (0)	0 (0)
ADD	-0.0057 (0.0035)	-0.0034 (0.0038)	-0.0001 (0.0001)	-0.0171 (0.0069)	-0.0001 (0.0002)	-0.0049 (0.0017)	-0.0002 (0.0001)	-0.0002 (0.0001)
GMAX	-0.0307 (0.0238)	0 (0)	-0.0007 (0.0024)	-0.0019 (0.0031)	-0.0026 (0.0016)	-0.0011 (0.0009)	-0.0008 (0.0004)	0 (0)
QF	-0.004 (0.0036)	0 (0)	0 (0)	-0.0038 (0.0029)	-0.0005 (0.0006)	-0.0001 (0.0001)	0 (0)	0 (0)
RF	0 (0)	-0.0579 (0.0138)	-0.0118 (0.0078)	-0.0069 (0.0062)	0 (0)	0 (0)	-0.0001 (0.0001)	0 (0)
VAS	0 (0)	0 (0)	0 (0)	-0.0004 (0.0007)	-0.0028 (0.0035)	0 (0.0001)	-0.0011 (0.0009)	0 (0)
GAS	0 (0)	-0.0107 (0.0024)	0 (0)	0 (0)	0 (0)	0 (0)	0 (0)	0 (0)
SOL	0 (0)	-0.0057 (0.0037)	0 (0)	0 (0)	0 (0)	0 (0)	0 (0)	0 (0)
ERCSPN	0 (0)	-0.1335 (0.0203)	0 (0)	-0.1162 (0.0302)	0 (0)	-0.0008 (0.0014)	0 (0)	0 (0)
INTBL	-0.019 (0.0112)	0 (0)	0 (0)	-0.0072 (0.0042)	0 (0)	-0.0018 (0.001)	0 (0)	-0.0003 (0.0002)
AO	-0.0089 (0.0055)	-0.007 (0.0063)	-0.0061 (0.007)	-0.0112 (0.0141)	-0.001 (0.0014)	-0.0013 (0.0018)	-0.0003 (0.0003)	-0.0003 (0.0002)

Table A.2: Men 0% 1RM: Normalized negative energy flows and standard deviation.

	barbell + torso	**pelvis**	**femur r**	**femur l**	**tibia r**	**tibia l**	**foot r**	**foot l**
HAM	0 (0)	0.1376 (0.0259)	0.0683 (0.0168)	0.0339 (0.0131)	0.0005 (0.0011)	0.0002 (0.0003)	0 (0)	0 (0)
BFSH	0 (0)	0 (0)	0 (0)	0.0002 (0.0002)	0 (0)	0.0001 (0.0001)	0.0002 (0.0001)	0 (0)
SAR	0.0069 (0.0035)	0 (0)	0 (0)	0 (0)	0 (0)	0.0001 (0.0001)	0 (0.0001)	0 (0)
ADD	0.0042 (0.0041)	0.026 (0.007)	0.0238 (0.0066)	0.0015 (0.0016)	0.0031 (0.0017)	0 (0)	0.0001 (0.0001)	0 (0)
GMAX	0.0032 (0.0038)	0.0732 (0.0135)	0.0388 (0.01)	0.0145 (0.0046)	0.0002 (0.0004)	0.0007 (0.0005)	0 (0)	0.0001 (0.0001)
QF	0 (0)	0.0213 (0.0081)	0.0252 (0.0095)	0 (0)	0.0008 (0.0005)	0.0001 (0.0001)	0 (0)	0 (0)
RF	0.0899 (0.0353)	0 (0)	0 (0)	0 (0)	0.0016 (0.0009)	0.0012 (0.0008)	0 (0)	0.0002 (0.0001)
VAS	0.1299 (0.0188)	0.0494 (0.0084)	0.0205 (0.0059)	0 (0)	0 (0.0001)	0 (0.0001)	0 (0)	0.0001 (0)
GAS	0.017 (0.0075)	0 (0)	0.0103 (0.0039)	0.001 (0.001)	0.0037 (0.0034)	0.0002 (0.0002)	0.0043 (0.0017)	0 (0)
SOL	0.021 (0.0041)	0 (0)	0.016 (0.0075)	0.0019 (0.0013)	0.0074 (0.0041)	0.0002 (0.0001)	0.004 (0.0014)	0 (0)
ERCSPN	0.3842 (0.1048)	0 (0)	0.0304 (0.0125)	0 (0)	0.0025 (0.0022)	0.0003 (0.0008)	0.0001 (0.0001)	0.0005 (0.0004)
INTBL	0 (0)	0.004 (0.0031)	0.0074 (0.0049)	0 (0)	0.0014 (0.001)	0 (0)	0.0002 (0.0002)	0 (0)
AO	0.0276 (0.0125)	0.0047 (0.0073)	0.0197 (0.0138)	0.0084 (0.0054)	0.0044 (0.0016)	0.0034 (0.0013)	0.001 (0.0003)	0.0009 (0.0003)

Table A.3: Men 25% 1RM: Normalized positive energy flows and standard deviation.

	barbell + torso	pelvis	femur r	femur l	tibia r	tibia l	foot r	foot l
HAM	-0.168 (0.0475)	0 (0)	0 (0)	0 (0)	-0.002 (0.0017)	-0.0017 (0.0014)	-0.0008 (0.0004)	-0.0003 (0.0001)
BFSH	-0.0036 (0.0029)	-0.0037 (0.0017)	-0.0037 (0.0017)	0 (0)	-0.0012 (0.0007)	0 (0)	0 (0)	0 (0)
SAR	-0.0004 (0.0007)	-0.0063 (0.0026)	-0.0045 (0.0023)	-0.001 (0.0008)	-0.0009 (0.0007)	0 (0.0001)	0 (0)	0 (0)
ADD	-0.0203 (0.0062)	-0.0045 (0.004)	-0.0001 (0.0003)	-0.0126 (0.0066)	-0.0001 (0.0002)	-0.004 (0.0021)	-0.0003 (0.0002)	-0.0002 (0.0001)
GMAX	-0.0591 (0.0233)	0 (0)	0 (0)	0 (0)	-0.0013 (0.001)	-0.0005 (0.0005)	-0.0007 (0.0002)	0 (0)
QF	-0.0188 (0.0078)	0 (0)	0 (0)	-0.0043 (0.0029)	0 (0)	0 (0.0001)	0 (0)	0 (0)
RF	0 (0)	-0.0439 (0.016)	-0.0162 (0.0096)	-0.0117 (0.0071)	0 (0)	-0.0002 (0.0006)	-0.0002 (0.0001)	0 (0)
VAS	0 (0)	0 (0)	0 (0)	-0.0055 (0.0035)	-0.0035 (0.0035)	-0.0003 (0.0003)	-0.0015 (0.0009)	0 (0)
GAS	0 (0)	-0.0115 (0.0019)	0 (0)	-0.0002 (0.0005)	-0.0001 (0.0006)	0 (0.0001)	0 (0)	0 (0)
SOL	0 (0)	-0.0124 (0.0032)	0 (0)	0 (0)	0 (0)	0 (0.0001)	0 (0)	0 (0)
ERCSPN	0 (0)	-0.1718 (0.0373)	0 (0)	-0.1763 (0.0414)	0 (0.0001)	-0.0033 (0.0017)	-0.0001 (0.0001)	0 (0.0001)
INTBL	-0.0108 (0.0088)	0 (0)	0 (0)	-0.0034 (0.0021)	0 (0)	-0.0008 (0.0006)	0 (0)	-0.0001 (0.0001)
AO	-0.01 (0.0091)	-0.0192 (0.0128)	-0.006 (0.0063)	-0.0173 (0.0088)	-0.0003 (0.0004)	-0.0017 (0.0012)	-0.0001 (0)	-0.0002 (0.0002)

Table A.4: Men 25% 1RM: Normalized negative energy flows and standard deviation.

	barbell + torso	pelvis	femur r	femur l	tibia r	tibia l	foot r	foot l
HAM	0 (0)	0.1231 (0.0328)	0.0652 (0.0108)	0.0339 (0.0117)	0.0007 (0.0009)	0.0005 (0.0006)	0 (0)	0 (0)
BFSH	0 (0)	0 (0)	0 (0)	0.0001 (0.0001)	0 (0)	0 (0.0001)	0 (0.0001)	0 (0)
SAR	0.0037 (0.0021)	0 (0)	0 (0)	0 (0)	0 (0)	0.0001 (0.0001)	0 (0)	0 (0)
ADD	0.0073 (0.004)	0.0253 (0.0098)	0.0236 (0.0085)	0.0013 (0.0018)	0.0032 (0.0016)	0 (0.0001)	0.0001 (0.0001)	0 (0)
GMAX	0.0039 (0.0055)	0.0741 (0.0156)	0.0441 (0.0101)	0.0156 (0.0051)	0.0002 (0.0002)	0.0006 (0.0003)	0 (0)	0 (0)
QF	0.0002 (0.0004)	0.0216 (0.0093)	0.0279 (0.0126)	0 (0)	0.0008 (0.0007)	0.0001 (0.0001)	0 (0)	0 (0)
RF	0.0884 (0.0492)	0 (0)	0 (0)	0 (0)	0.001 (0.0009)	0.0008 (0.0008)	0 (0)	0.0001 (0.0001)
VAS	0.1413 (0.0144)	0.0466 (0.0148)	0.0229 (0.0141)	0 (0)	0.0003 (0.0008)	0 (0)	0 (0)	0.0001 (0)
GAS	0.0166 (0.0082)	0 (0)	0.0051 (0.0031)	0.0003 (0.0003)	0.0013 (0.0013)	0.0001 (0.0001)	0.0032 (0.0009)	0 (0)
SOL	0.0313 (0.0073)	0 (0)	0.0167 (0.0132)	0.0011 (0.0012)	0.0073 (0.0051)	0.0001 (0.0001)	0.004 (0.0018)	0 (0)
ERCSPN	0.4134 (0.126)	0 (0)	0.0213 (0.0184)	0 (0)	0.002 (0.0022)	0 (0)	0.0001 (0.0002)	0.0003 (0.0002)
INTBL	0 (0)	0.0025 (0.0016)	0.0056 (0.0044)	0 (0)	0.0012 (0.0012)	0 (0)	0.0001 (0.0002)	0 (0)
AO	0.0393 (0.026)	0.0072 (0.0075)	0.0251 (0.0196)	0.0105 (0.0061)	0.0045 (0.0026)	0.0032 (0.0018)	0.001 (0.0004)	0.0009 (0.0005)

Table A.5: Men 40% 1RM: Normalized positive energy flows and standard deviation.

	barbell + torso	pelvis	femur r	femur l	tibia r	tibia l	foot r	foot l
HAM	-0.164 (0.0526)	0 (0)	0 (0)	0 (0)	-0.0014 (0.002)	-0.0011 (0.0009)	-0.0006 (0.0004)	-0.0001 (0.0001)
BFSH	-0.0015 (0.0015)	-0.0016 (0.0011)	-0.0017 (0.0009)	0 (0)	-0.0005 (0.0004)	0 (0)	0 (0)	0 (0)
SAR	-0.0004 (0.0007)	-0.0032 (0.0027)	-0.0022 (0.0015)	-0.0007 (0.0007)	-0.0003 (0.0003)	0 (0)	0 (0)	0 (0)
ADD	-0.0235 (0.0082)	-0.0058 (0.0029)	-0.0006 (0.0005)	-0.0119 (0.0037)	0 (0)	-0.004 (0.0014)	-0.0003 (0.0002)	-0.0002 (0.0001)
GMAX	-0.0705 (0.026)	0 (0)	0 (0)	0 (0)	-0.0009 (0.001)	-0.0004 (0.0004)	-0.0005 (0.0002)	0 (0)
QF	-0.0215 (0.0064)	0 (0)	0 (0)	-0.0056 (0.004)	0 (0.0001)	0 (0.0001)	-0.0001 (0)	0 (0)
RF	0 (0)	-0.0407 (0.0229)	-0.0193 (0.0145)	-0.0126 (0.008)	0 (0)	-0.0002 (0.0005)	-0.0001 (0.0001)	0 (0)
VAS	0 (0)	0 (0)	0 (0)	-0.0085 (0.0044)	-0.0027 (0.0021)	-0.0007 (0.0005)	-0.0014 (0.0007)	0 (0)
GAS	0 (0)	-0.0104 (0.0022)	0 (0)	-0.0004 (0.0005)	-0.0002 (0.0004)	-0.0001 (0.0001)	0 (0)	0 (0)
SOL	0 (0)	-0.0161 (0.0058)	0 (0)	-0.0001 (0.0002)	0 (0)	-0.0001 (0.0001)	0 (0)	0 (0)
ERCSPN	0 (0)	-0.1761 (0.0406)	-0.0027 (0.0059)	-0.1845 (0.0465)	-0.0001 (0.0002)	-0.0049 (0.0034)	-0.0001 (0.0002)	-0.0001 (0.0001)
INTBL	-0.0088 (0.006)	0 (0)	0 (0)	-0.0024 (0.002)	0 (0)	-0.0006 (0.0005)	0 (0)	-0.0001 (0.0001)
AO	-0.0237 (0.0277)	-0.0227 (0.0168)	-0.0114 (0.0104)	-0.0233 (0.0145)	-0.0004 (0.0003)	-0.002 (0.002)	0 (0)	-0.0001 (0.0001)

Table A.6: Men 40% 1RM: Normalized negative energy flows and standard deviation.

	barbell + torso	pelvis	femur r	femur l	tibia r	tibia l	foot r	foot l
HAM	0 (0)	0.1242 (0.0308)	0.0372 (0.0092)	0.0063 (0.0075)	0 (0.0001)	0 (0.0001)	0 (0)	0 (0)
BFSH	0 (0)	0 (0)	0 (0)	0 (0)	0 (0)	0 (0)	0.0002 (0.0001)	0 (0)
SAR	0.0018 (0.0015)	0 (0)	0 (0)	0.0006 (0.0012)	0 (0)	0.0014 (0.001)	0.0002 (0.0001)	0.0001 (0.0001)
ADD	0.003 (0.0032)	0.0282 (0.0057)	0.0323 (0.0049)	0.0001 (0.0002)	0.0053 (0.0015)	0 (0)	0.0001 (0.0001)	0 (0)
GMAX	0.0025 (0.0047)	0.0659 (0.0109)	0.0257 (0.0051)	0.0063 (0.0034)	0 (0)	0.0005 (0.0003)	0 (0)	0 (0)
QF	0.0025 (0.0038)	0.0246 (0.008)	0.0185 (0.0083)	0 (0)	0 (0.0001)	0.0001 (0.0001)	0 (0)	0 (0)
RF	0.0937 (0.0325)	0 (0)	0 (0)	0.0025 (0.0054)	0.0076 (0.0034)	0.0072 (0.0031)	0.0001 (0)	0.0005 (0.0002)
VAS	0.0868 (0.0153)	0.0468 (0.0068)	0.0306 (0.0085)	0.004 (0.0021)	0.0026 (0.0016)	0.0003 (0.0001)	0 (0)	0 (0)
GAS	0.0098 (0.0069)	0 (0)	0.0106 (0.005)	0.0019 (0.0007)	0.0031 (0.0026)	0.0007 (0.0003)	0.0044 (0.0016)	0.0001 (0)
SOL	0.0107 (0.0027)	0.0001 (0.0002)	0.0084 (0.0044)	0.0016 (0.0008)	0.0021 (0.0015)	0.0003 (0.0001)	0.0017 (0.0006)	0 (0)
ERCSPN	0.2465 (0.026)	0 (0)	0.0393 (0.0113)	0 (0)	0.0042 (0.0014)	0.002 (0.0018)	0.0001 (0.0001)	0.0001 (0.0001)
INTBL	0 (0)	0.0129 (0.0055)	0.0177 (0.0066)	0 (0)	0.0026 (0.0016)	0 (0)	0.0003 (0.0003)	0 (0)
AO	0.0141 (0.0096)	0.0061 (0.0081)	0.0155 (0.0071)	0.0154 (0.0083)	0.0044 (0.0016)	0.0042 (0.0013)	0.0014 (0.0004)	0.0012 (0.0004)

Table A.7: Women 0% 1RM: Normalized positive energy flows and standard deviation.

	barbell + torso	**pelvis**	**femur r**	**femur l**	**tibia r**	**tibia l**	**foot r**	**foot l**
HAM	-0.0658 (0.0275)	0 (0)	0 (0)	-0.004 (0.0086)	-0.006 (0.0021)	-0.007 (0.0032)	-0.0006 (0.0003)	-0.0003 (0.0002)
BFSH	-0.0039 (0.0017)	-0.0038 (0.0016)	-0.0036 (0.0019)	-0.0001 (0.0001)	-0.0013 (0.0011)	0 (0)	0 (0)	0 (0)
SAR	-0.0008 (0.0018)	-0.0198 (0.0139)	-0.0101 (0.0084)	-0.0006 (0.0009)	-0.0009 (0.001)	0 (0)	0 (0)	0 (0)
ADD	-0.0043 (0.0047)	-0.0024 (0.0021)	0 (0.0001)	-0.0238 (0.0066)	0 (0)	-0.0072 (0.0018)	-0.0002 (0.0001)	-0.0003 (0.0002)
GMAX	-0.0077 (0.007)	0 (0)	0 (0)	-0.0032 (0.0038)	-0.0021 (0.0009)	-0.0021 (0.0007)	-0.0005 (0.0003)	0 (0)
QF	-0.0028 (0.0033)	0 (0)	0 (0)	-0.0059 (0.002)	-0.0009 (0.0009)	-0.0001 (0.0001)	0 (0)	0 (0)
RF	0 (0)	-0.077 (0.0268)	-0.0116 (0.0061)	-0.0047 (0.0061)	0 (0)	0 (0)	0 (0)	0 (0)
VAS	0 (0)	0 (0)	0 (0)	0 (0)	-0.0001 (0.0002)	0 (0)	-0.0003 (0.0003)	0 (0)
GAS	-0.0001 (0.0003)	-0.0073 (0.0027)	-0.0001 (0.0002)	0 (0)	-0.0003 (0.0007)	0 (0)	0 (0)	0 (0)
SOL	0 (0)	-0.0013 (0.0016)	0 (0)	0 (0)	0 (0)	0 (0)	0 (0)	0 (0)
ERCSPN	0 (0)	-0.1113 (0.0177)	0 (0)	-0.0903 (0.0195)	0 (0)	0 (0.0001)	0 (0)	0 (0)
INTBL	-0.0251 (0.0105)	0 (0)	0 (0)	-0.0089 (0.003)	0 (0)	-0.0018 (0.0006)	0 (0)	-0.0004 (0.0002)
AO	-0.009 (0.0067)	-0.0105 (0.0104)	-0.0068 (0.0081)	-0.0062 (0.0059)	-0.0007 (0.0008)	-0.0014 (0.0014)	-0.0002 (0.0002)	-0.0004 (0.0004)

Table A.8: Women 0% 1RM: Normalized negative energy flows and standard deviation.

	barbell + torso	**pelvis**	**femur r**	**femur l**	**tibia r**	**tibia l**	**foot r**	**foot l**
HAM	0.0062 (0.0105)	0.1154 (0.0206)	0.0462 (0.0113)	0.0175 (0.0092)	0.0001 (0.0001)	0.0001 (0.0001)	0 (0)	0 (0)
BFSH	0 (0)	0 (0)	0 (0)	0.0002 (0.0002)	0 (0)	0.0001 (0)	0.0002 (0.0001)	0 (0)
SAR	0.0039 (0.0029)	0 (0)	0 (0)	0.0002 (0.0004)	0 (0)	0.0003 (0.0003)	0.0001 (0.0001)	0.0001 (0)
ADD	0.0056 (0.0054)	0.0267 (0.0072)	0.0286 (0.0082)	0.0005 (0.0008)	0.0037 (0.0015)	0 (0)	0.0001 (0.0001)	0 (0)
GMAX	0.0127 (0.0105)	0.0648 (0.0102)	0.0281 (0.0071)	0.009 (0.0037)	0 (0)	0.0004 (0.0003)	0 (0)	0 (0)
QF	0.0016 (0.0023)	0.0225 (0.0076)	0.0223 (0.0077)	0 (0)	0.0002 (0.0003)	0.0001 (0.0001)	0 (0)	0 (0)
RF	0.0697 (0.0281)	0 (0)	0 (0.0001)	0.0005 (0.0011)	0.0033 (0.0015)	0.0033 (0.0016)	0 (0)	0.0003 (0.0001)
VAS	0.1295 (0.0203)	0.0384 (0.0071)	0.0204 (0.0073)	0 (0.0002)	0.0006 (0.0007)	0.0001 (0.0001)	0 (0)	0 (0)
GAS	0.0132 (0.0065)	0 (0)	0.0096 (0.0034)	0.001 (0.0008)	0.0044 (0.0019)	0.0004 (0.0001)	0.0055 (0.0013)	0 (0)
SOL	0.0219 (0.005)	0 (0)	0.0169 (0.0046)	0.0014 (0.0007)	0.0067 (0.0025)	0.0003 (0.0001)	0.0035 (0.0013)	0 (0)
ERCSPN	0.3113 (0.0677)	0 (0)	0.0344 (0.0147)	0 (0)	0.0054 (0.0025)	0.0006 (0.001)	0.0002 (0.0002)	0.0003 (0.0002)
INTBL	0.0001 (0.0004)	0.0082 (0.0059)	0.0119 (0.0083)	0 (0)	0.0011 (0.0011)	0 (0)	0.0002 (0.0003)	0 (0)
AO	0.0256 (0.0189)	0.0075 (0.0065)	0.0146 (0.0078)	0.0143 (0.0095)	0.0037 (0.0013)	0.0035 (0.0013)	0.0009 (0.0003)	0.0008 (0.0003)

Table A.9: Women 25% 1RM: Normalized positive energy flows and standard deviation.

	barbell + torso	**pelvis**	**femur r**	**femur l**	**tibia r**	**tibia l**	**foot r**	**foot l**
HAM	-0.1081 (0.0229)	0 (0)	0 (0)	-0.0003 (0.0009)	-0.0044 (0.0014)	-0.0042 (0.0018)	-0.0008 (0.0002)	-0.0003 (0.0002)
BFSH	-0.0031 (0.0013)	-0.0022 (0.0012)	-0.0023 (0.0012)	0 (0)	-0.0006 (0.0004)	0 (0)	0 (0)	0 (0)
SAR	-0.001 (0.0014)	-0.0062 (0.0046)	-0.0035 (0.0029)	-0.0006 (0.0006)	-0.0003 (0.0003)	0 (0)	0 (0)	0 (0)
ADD	-0.0171 (0.0069)	-0.0031 (0.0019)	0 (0.0001)	-0.0174 (0.0077)	-0.0001 (0.0002)	-0.0055 (0.0021)	-0.0003 (0.0002)	-0.0002 (0.0002)
GMAX	-0.0345 (0.0081)	0 (0)	0 (0.0001)	-0.0009 (0.002)	-0.0029 (0.0005)	-0.0014 (0.0006)	-0.0008 (0.0002)	0 (0)
QF	-0.0139 (0.0066)	0 (0)	0 (0)	-0.0049 (0.0034)	-0.0005 (0.0005)	0 (0.0001)	-0.0001 (0)	0 (0)
RF	-0.0006 (0.0012)	-0.0449 (0.018)	-0.0112 (0.0063)	-0.006 (0.0046)	0 (0)	0 (0)	0 (0.0001)	0 (0)
VAS	0 (0)	0 (0)	0 (0)	-0.0036 (0.0031)	-0.0013 (0.002)	-0.0002 (0.0002)	-0.0012 (0.0006)	0 (0)
GAS	0 (0)	-0.01 (0.0014)	0 (0)	-0.0001 (0.0002)	0 (0)	0 (0)	0 (0)	0 (0)
SOL	0 (0)	-0.0092 (0.0026)	0 (0)	0 (0)	0 (0)	0 (0)	0 (0)	0 (0)
ERCSPN	0 (0)	-0.149 (0.0338)	0 (0)	-0.1349 (0.0302)	0 (0)	-0.0012 (0.0017)	0 (0.0001)	0 (0.0001)
INTBL	-0.0172 (0.0123)	0 (0)	0 (0)	-0.0058 (0.0041)	0 (0)	-0.0009 (0.001)	0 (0)	-0.0002 (0.0003)
AO	-0.0132 (0.009)	-0.0101 (0.0133)	-0.0082 (0.0103)	-0.0081 (0.0094)	-0.0006 (0.001)	-0.0011 (0.0013)	-0.0002 (0.0002)	-0.0002 (0.0002)

Table A.10: Women 25% 1RM: Normalized negative energy flows and standard deviation.

	barbell + torso	**pelvis**	**femur r**	**femur l**	**tibia r**	**tibia l**	**foot r**	**foot l**
HAM	0.007 (0.0093)	0.1109 (0.0212)	0.0492 (0.0111)	0.0179 (0.0096)	0.0001 (0.0002)	0.0001 (0.0002)	0 (0)	0 (0)
BFSH	0 (0)	0 (0)	0 (0)	0.0002 (0.0001)	0 (0)	0.0001 (0)	0.0001 (0.0001)	0 (0)
SAR	0.0034 (0.0027)	0 (0)	0 (0)	0.0003 (0.0005)	0 (0)	0.0003 (0.0003)	0.0001 (0)	0 (0)
ADD	0.0105 (0.0072)	0.0295 (0.0108)	0.0314 (0.0114)	0.0005 (0.0013)	0.0043 (0.0019)	0 (0)	0.0002 (0.0001)	0 (0)
GMAX	0.0166 (0.0125)	0.0656 (0.011)	0.0315 (0.0099)	0.0085 (0.0042)	0.0001 (0.0002)	0.0004 (0.0003)	0 (0)	0 (0)
QF	0.0024 (0.003)	0.028 (0.0146)	0.0304 (0.0167)	0 (0)	0.0002 (0.0004)	0 (0.0001)	0 (0)	0 (0)
RF	0.0755 (0.0396)	0 (0)	0 (0)	0.0001 (0.0002)	0.003 (0.0019)	0.0027 (0.0016)	0 (0)	0.0003 (0.0001)
VAS	0.1393 (0.0268)	0.0336 (0.0064)	0.0177 (0.0074)	0 (0.0001)	0.0005 (0.0007)	0 (0.0001)	0 (0)	0 (0)
GAS	0.0131 (0.0074)	0 (0)	0.007 (0.0032)	0.0007 (0.0009)	0.0031 (0.0015)	0.0002 (0.0002)	0.005 (0.0013)	0 (0)
SOL	0.0286 (0.0082)	0 (0)	0.0173 (0.0062)	0.0013 (0.0014)	0.0069 (0.0029)	0.0002 (0.0001)	0.0038 (0.0015)	0 (0)
ERCSPN	0.3256 (0.0873)	0 (0)	0.0273 (0.0165)	0 (0)	0.0047 (0.0025)	0.0003 (0.0005)	0.0002 (0.0002)	0.0002 (0.0002)
INTBL	0.0001 (0.0002)	0.0081 (0.0086)	0.0122 (0.0121)	0 (0)	0.001 (0.001)	0 (0)	0.0002 (0.0002)	0 (0)
AO	0.0359 (0.0363)	0.006 (0.0038)	0.0126 (0.0085)	0.015 (0.0074)	0.004 (0.002)	0.0039 (0.0013)	0.0008 (0.0003)	0.0008 (0.0003)

Table A.11: Women 40% 1RM: Normalized positive energy flows and standard deviation.

	barbell + torso	**pelvis**	**femur r**	**femur l**	**tibia r**	**tibia l**	**foot r**	**foot l**
HAM	-0.1133 (0.0285)	0 (0)	0 (0)	-0.0002 (0.0008)	-0.0036 (0.0015)	-0.0035 (0.0017)	-0.0007 (0.0002)	-0.0002 (0.0001)
BFSH	-0.002 (0.0011)	-0.0014 (0.0008)	-0.0018 (0.0012)	0 (0)	-0.0006 (0.0005)	0 (0)	0 (0)	0 (0)
SAR	-0.0011 (0.0019)	-0.0049 (0.0042)	-0.0028 (0.0024)	-0.0005 (0.0009)	-0.0003 (0.0006)	0 (0)	0 (0)	0 (0)
ADD	-0.0214 (0.0074)	-0.0053 (0.0024)	-0.0001 (0.0005)	-0.0201 (0.0102)	0 (0.0001)	-0.0064 (0.0031)	-0.0003 (0.0002)	-0.0003 (0.0002)
GMAX	-0.0422 (0.0095)	0 (0)	0 (0)	-0.0012 (0.0026)	-0.0026 (0.0008)	-0.0014 (0.0007)	-0.0007 (0.0002)	-0.0001 (0)
QF	-0.0174 (0.0073)	0 (0)	0 (0)	-0.0083 (0.0065)	-0.0004 (0.0004)	-0.0001 (0.0001)	-0.0001 (0)	0 (0)
RF	-0.0001 (0.0005)	-0.0472 (0.0254)	-0.015 (0.0124)	-0.0064 (0.0079)	0 (0)	0 (0)	0 (0)	0 (0)
VAS	0 (0)	0 (0)	0 (0)	-0.0061 (0.0038)	-0.0012 (0.002)	-0.0003 (0.0003)	-0.0013 (0.0005)	0 (0)
GAS	0 (0)	-0.0108 (0.0022)	0 (0)	-0.0002 (0.0004)	0 (0.0001)	0 (0)	0 (0)	0 (0)
SOL	0 (0)	-0.0123 (0.0027)	0 (0)	-0.0002 (0.0003)	0 (0)	0 (0.0001)	0 (0)	0 (0)
ERCSPN	0 (0)	-0.1486 (0.0357)	-0.0009 (0.004)	-0.1395 (0.0328)	0 (0.0002)	-0.0017 (0.0024)	0 (0)	-0.0001 (0.0001)
INTBL	-0.0175 (0.0184)	0 (0)	0 (0)	-0.0063 (0.0067)	0 (0.0001)	-0.0008 (0.0009)	0 (0)	-0.0002 (0.0002)
AO	-0.0138 (0.0112)	-0.0137 (0.0188)	-0.0114 (0.0112)	-0.0098 (0.0146)	-0.0008 (0.0009)	-0.001 (0.0013)	-0.0001 (0.0001)	-0.0002 (0.0002)

Table A.12: Women 40% 1RM: Normalized negative energy flows and standard deviation.

Bibliography

Anderson, Frank C., & Pandy, Marcus G. 2001. Static and dynamic optimization solutions for gait are practically equivalent. *Journal of Biomechanics*, **34**(2), 153–161.

Bobbert, Maarten F., & van Ingen Schenau, Gerrit Jan. 1988. Coordination in vertical jumping. *Journal of Biomechanics*, **21**(3), 249–262.

Bobbert, Maarten F., & van Zandwijk, Jan Peter. 1994. Dependence of human maximum jump height on moment arms of the bi-articular m. gastrocnemius; a simulation study. *Human Movement Science*, **13**(5), 697–716.

Bobbert, Maarten F., Huijing, Peter A., & van Ingen Schenau, Gerrit Jan. 1986. An estimation of power output and work done by the human triceps surae musle-tendon complex in jumping. *Journal of Biomechanics*, **19**(11), 899–906.

Bosco, C., Viitasalo, J. T., Komi, P. V., & Luhtanen, P. 1982. Combined effect of elastic energy and myoelectrical potentiation during stretch-shortening cycle exercise. *Acta Physiologica Scandinavica*, **114**(4), 557–565.

Delp, S.L., Anderson, F.C., Arnold, AS., Loan, P., Habib, A, John, C.T., Guendelman, E., & Thelen, D.G. 2007. OpenSim: Open-Source Software to

Create and Analyze Dynamic Simulations of Movement. *IEEE Transactions on Biomedical Engineering*, **54**(11), 1940–1950.

Dorn, Tim W., Lin, Yi-Chung, & Pandy, Marcus G. 2012a. Estimates of muscle function in human gait depend on how foot-ground contact is modelled. *Computer Methods in Biomechanics and Biomedical Engineering*, **15**(6), 657–668.

Dorn, Tim W., Schache, Anthony G., & Pandy, Marcus G. 2012b. Muscular strategy shift in human running: dependence of running speed on hip and ankle muscle performance. *The Journal of Experimental Biology*, **215**(11), 1944–1956.

Fregly, Benjamin J., & Zajac, Felix E. 1996. A state-space analysis of mechanical energy generation, absorption, and transfer during pedaling. *Journal of Biomechanics*, **29**(1), 81–90.

Frontera, W. R., Hughes, V. A., Lutz, K. J., & Evans, W. J. 1991. A cross-sectional study of muscle strength and mass in 45- to 78-yr-old men and women. *Journal of Applied Physiology (Bethesda, Md.: 1985)*, **71**(2), 644–650.

Gregoire, L., Veeger, H., Huijing, P., & van Ingen Schenau, G. 1984. Role of Mono- and Biarticular Muscles in Explosive Movements. *International Journal of Sports Medicine*, **05**(06), 301–305.

Hamner, Samuel R., Seth, Ajay, & Delp, Scott L. 2010. Muscle contributions to propulsion and support during running. *Journal of Biomechanics*, **43**(14), 2709–2716.

Jacobs, Ron, Bobbert, Maarten F., & van Ingen Schenau, Gerrit Jan. 1996. Mechanical output from individual muscles during explosive leg extensions: The role of biarticular muscles. *Journal of Biomechanics*, **29**(4), 513–523.

Kanehisa, H., Ikegawa, S., & Fukunaga, T. 1994. Comparison of muscle cross-sectional area and strength between untrained women and men. *European Journal of Applied Physiology and Occupational Physiology*, **68**(2), 148–154.

Lin, Yi-Chung, Kim, Hyung Joo, & Pandy, Marcus G. 2011. A computationally efficient method for assessing muscle function during human locomotion. *International Journal for Numerical Methods in Biomedical Engineering*, **27**(3), 436–449.

Pandy, Marcus G., & Zajac, Felix E. 1991. Optimal muscular coordination strategies for jumping. *Journal of Biomechanics*, **24**(1), 1–10.

Prilutsky, Boris I., & Zatsiorsky, Vladimir M. 1994. Tendon action of two-joint muscles: transfer of mechanical energy between joints during jumping, landing, and running. *Journal of biomechanics*, **27**(1), 2534.

Schenau, G. J. van Ingen, Bobbert, M. F., & Rozendal, R. H. 1987. The unique action of bi-articular muscles in complex movements. *Journal of Anatomy*, **155**(Dec.), 1.

Van Ingen Schenau, Gerrit Jan. 1989. From rotation to translation: Constraints on multi-joint movements and the unique action of bi-articular muscles. *Human Movement Science*, **8**(4), 301–337.

van Soest, Arthur J., & Bobbert, Maarten F. 1993. The contribution of muscle properties in the control of explosive movements. *Biological cybernetics*, **69**(3), 195204.

van Soest, Arthur J., Schwab, Arend L., Bobbert, Maarten F., & van Ingen Schenau, Gerrit Jan. 1993. The influence of the biarticularity of the gastrocnemius muscle on vertical-jumping achievement. *Journal of Biomechanics*, **26**(1), 1–8.

Vos, E. J., Mullender, M. G., & Schenau, G. J. van Ingen. 1990. Electromechanical delay in the vastus lateralis muscle during dynamic isometric contractions. *European Journal of Applied Physiology and Occupational Physiology*, **60**(6), 467–471.

Vita

Stephen Douglas Riutta graduated magna cum laude with a B.S. mechanical engineering and a B.S. in biomedical engineering from Michigan Technological University. As an undergraduate, he conducted research at Clemson University and Princeton University through the Research Experience for Undergraduates program sponsored by the National Science Foundation. Upon graduating from Michigan Tech, Mr. Riutta served as a math and science teacher through the Peace Corps for two years in the West African country of Ghana. Upon returning to the US, he worked as a full-time engineering intern for eight months at Kimberly-Clark in Fullerton, California. After completing the internship, he began his graduate studies in the mechanical engineering department of The University of Texas at Austin. Upon the completion of his graduate studies at The University of Texas at Austin, he will study medicine at the University of Michigan Medical School. He can be contacted at `sdriutta@gmail.com`.

This thesis was typeset by the author.